

ME Supervisors' Mtg

Joe Silber

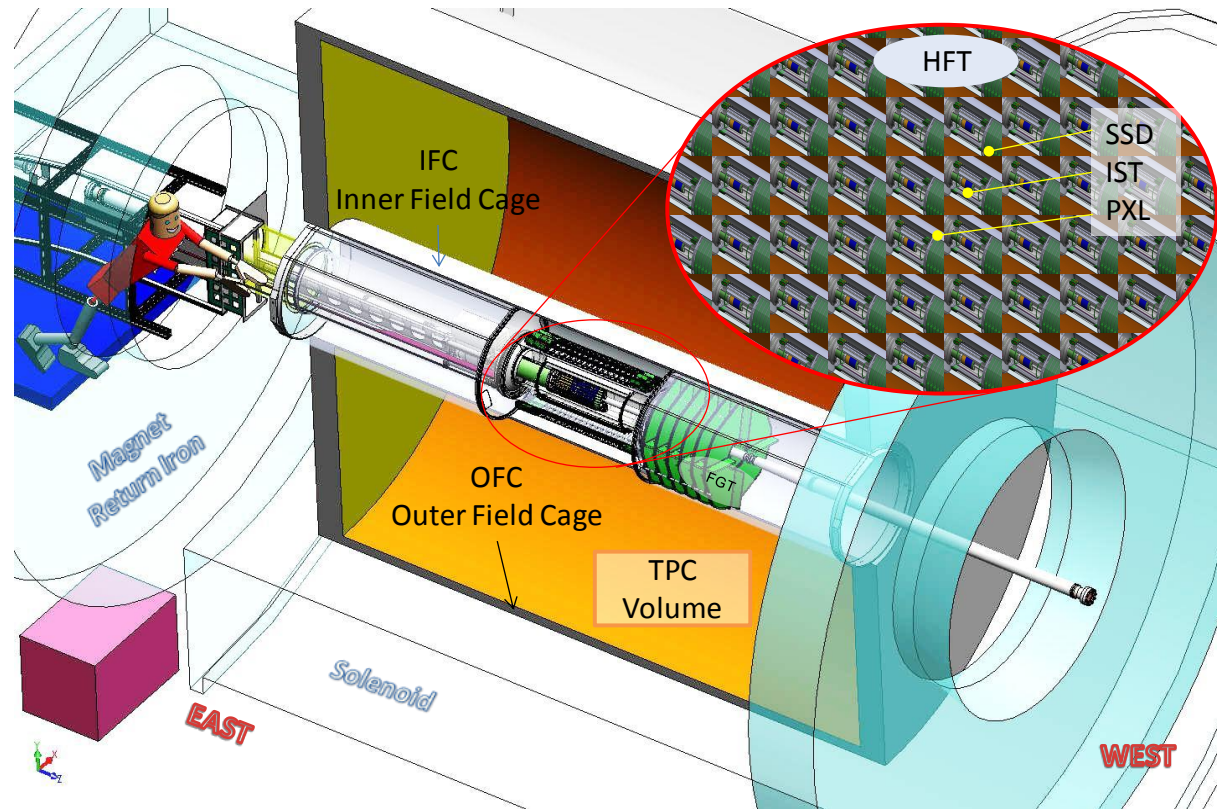
2012-04-12

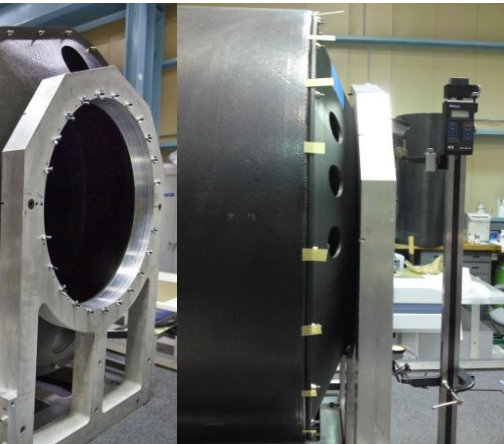
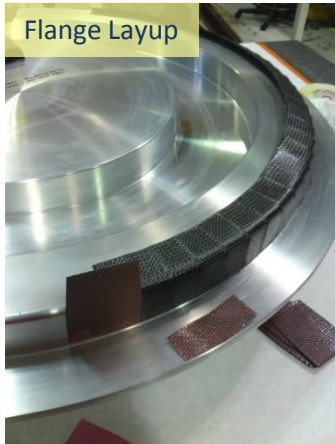
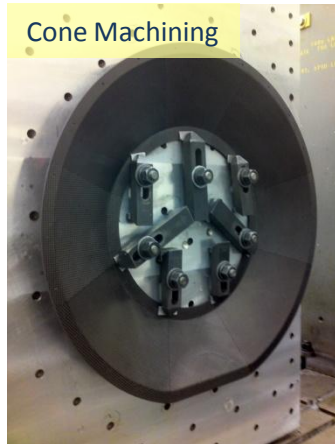
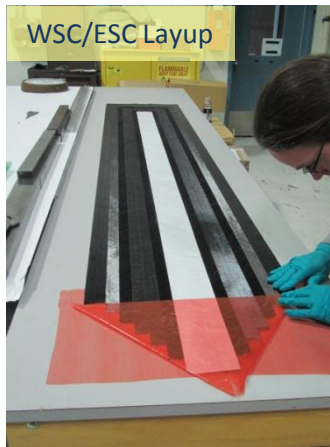
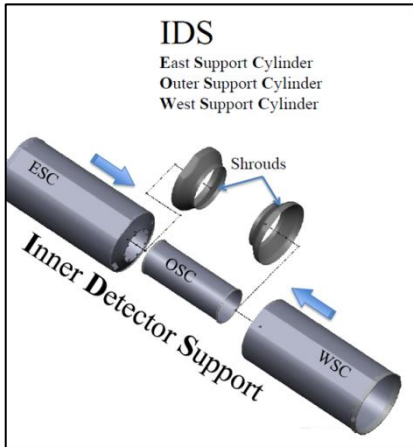
About me

- At LBNL now for 2 yrs. Main projects:
 - STAR HFT ~60%
 - ATLAS Upgrade ~10%
 - BigBOSS ~30%
- Grad work was in composite materials
- Built race cars at Cal
- Before then worked in structural engineering (small bridges/underpasses) and product design (electronic bike lockers)
- Ages ago did bachelor's in Studio Art

STAR HFT

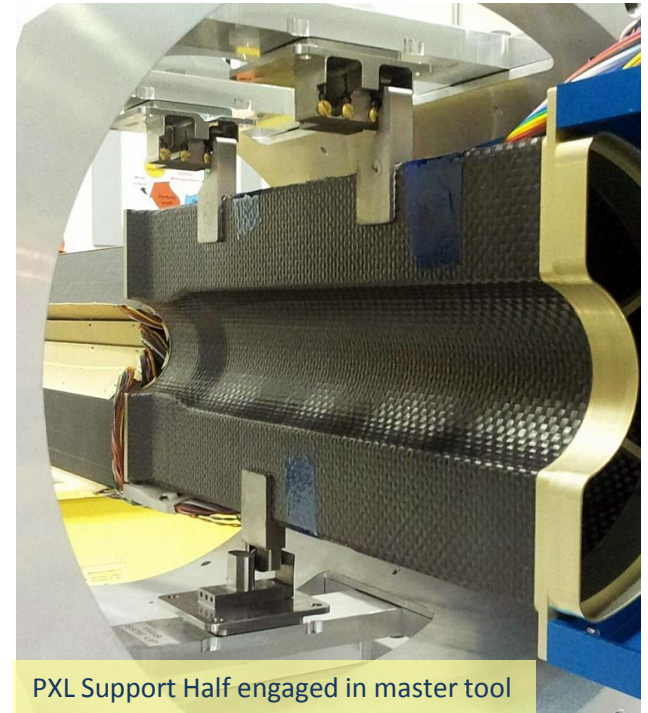
- HFT is a new inner tracking system for STAR, with 4 layers of silicon and 6 gem disks
- Timeline:
 - @ CD1 when I was hired in Mar 2010
 - CD2/3 was in mid 2011
 - Nov 2011 main support structures + FGT were installed
 - July-Dec 2012 PXL support and PXL for engineering run
 - Summer 2013 full PXL + IST + SSD
- Key component is PXL:
 - 2 innermost silicon layers
 - Truly rapid insertion/removal
 - Very low mass
 - TPC is great; PXL will much improve pointing
- At LBL we're building:
 - All the support structure (IDS)
 - All of PXL
 - IST local supports
- My role is to support Eric A. with structural analysis, material testing, detail design, tooling, production
- Complex assembly of carbon reinforced composite parts



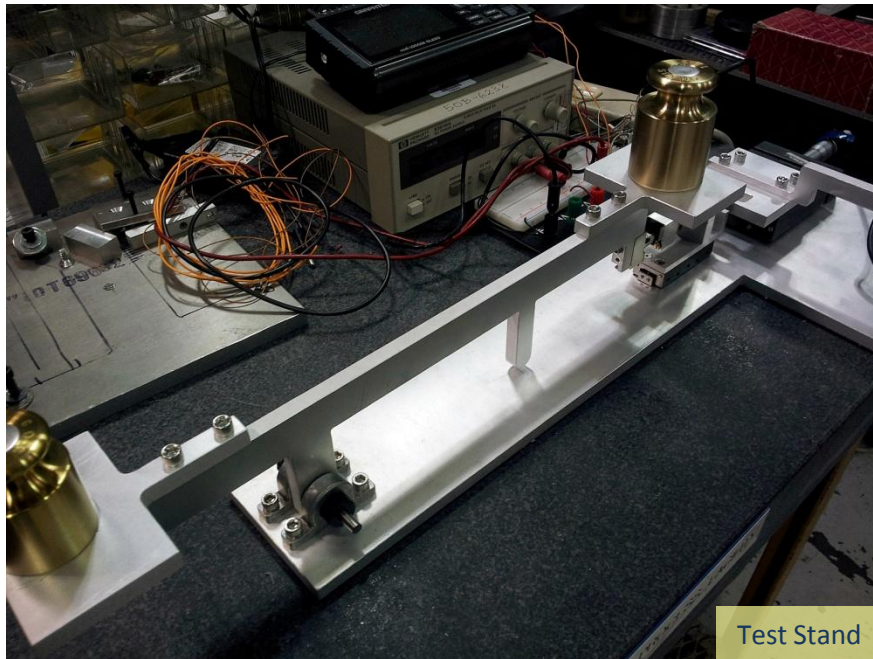


STAR PXL Kinematic Mounts

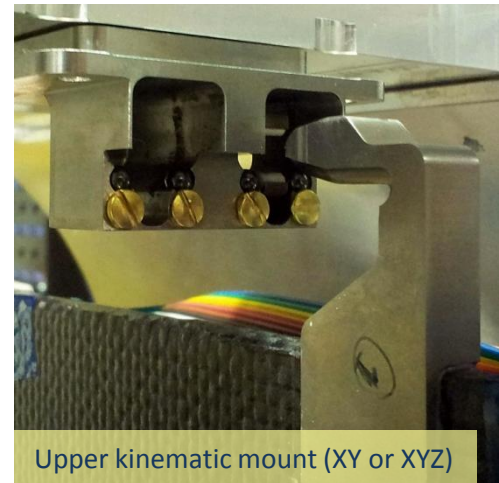
- Design constraints
 - 50 μ m positioning repeatability for all parts (6x detector halves)
 - Insertion is remote (detector tracks in \sim 3m along circuitous route before engaging mount); no tool access
 - Confined space, low mass, nothing magnetic
 - High enough retention force to keep detector stably located, but low enough to insert/remove detector without significant impact
- One could design a mechanism with rotating components, i.e., cams and locks; I chose the other route, to make it a flexures-with-friction problem. This allows:
 - Simple FBD analysis (as long as you test μ first!)
 - Accurate spring stiffnesses machined-in to parts by design



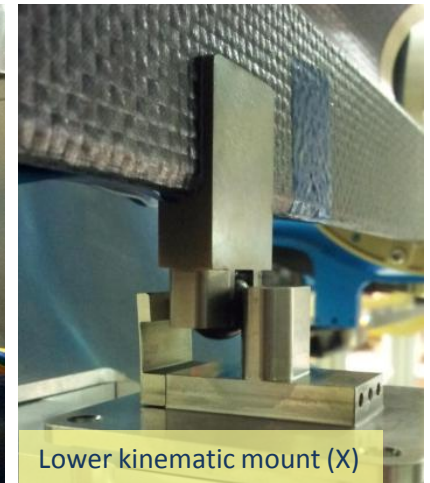
PXL Support Half engaged in master tool



Test Stand

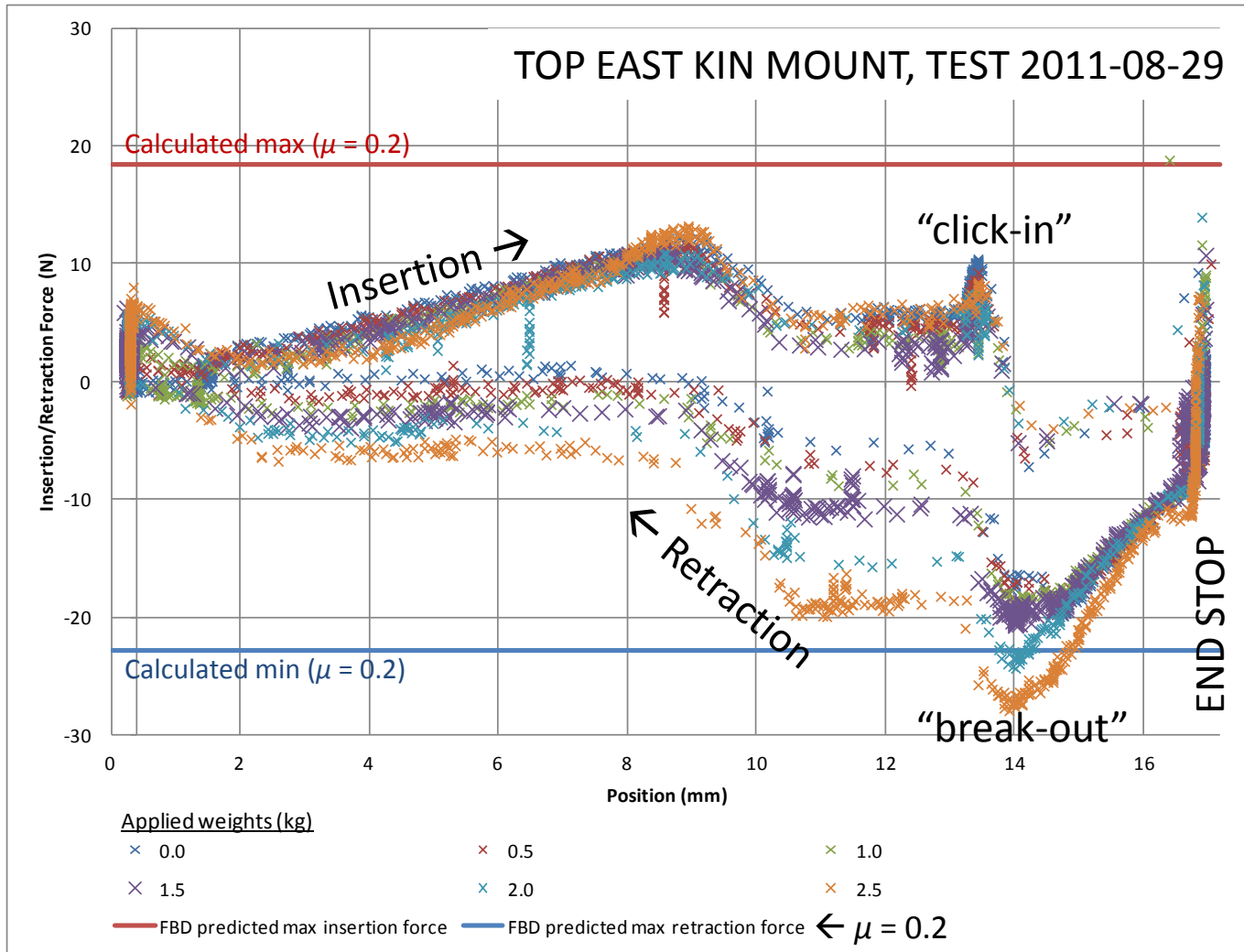


Upper kinematic mount (XY or XYZ)



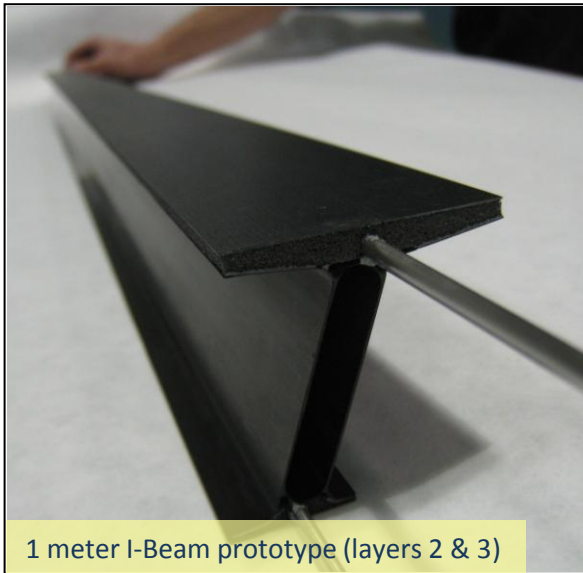
Lower kinematic mount (X)

STAR PXL Kinematic Mounts Force-Disp Results on Test Stand

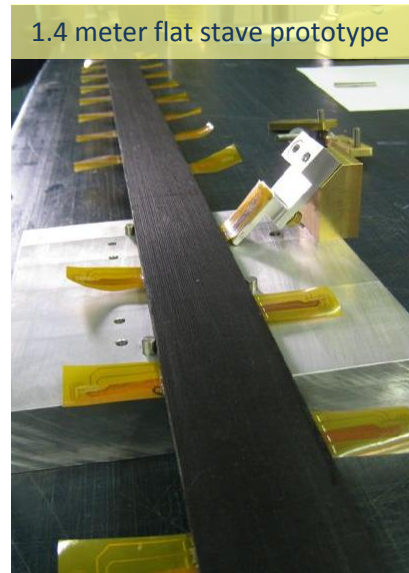
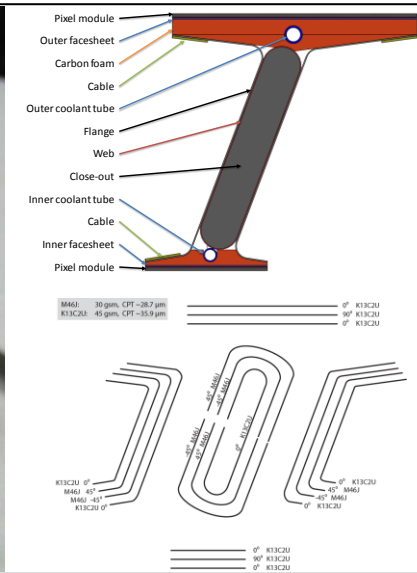


ATLAS Upgrade

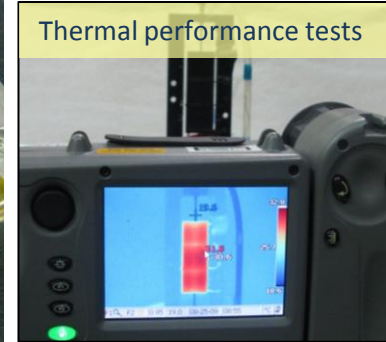
Local support beams, R&D on materials, tooling, and fabrication techniques



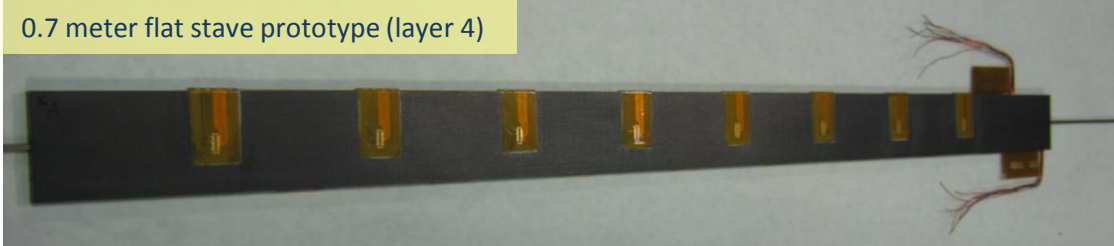
1 meter I-Beam prototype (layers 2 & 3)



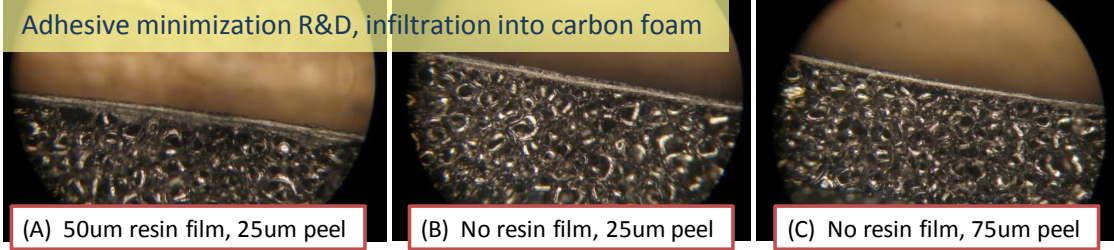
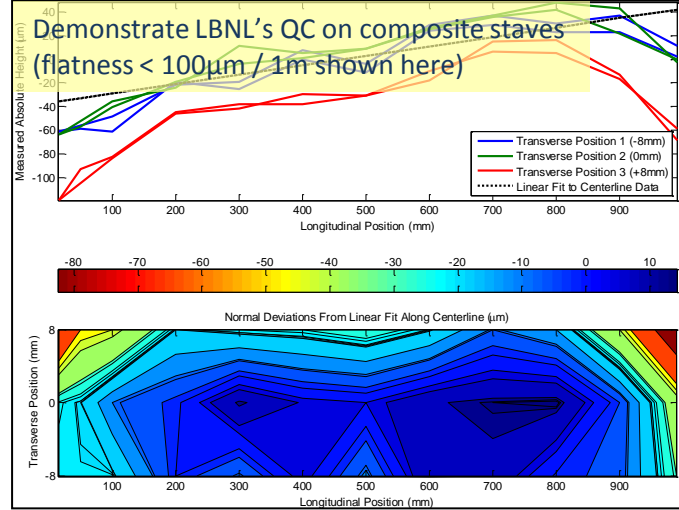
1.4 meter flat stave prototype



Thermal performance tests



0.7 meter flat stave prototype (layer 4)

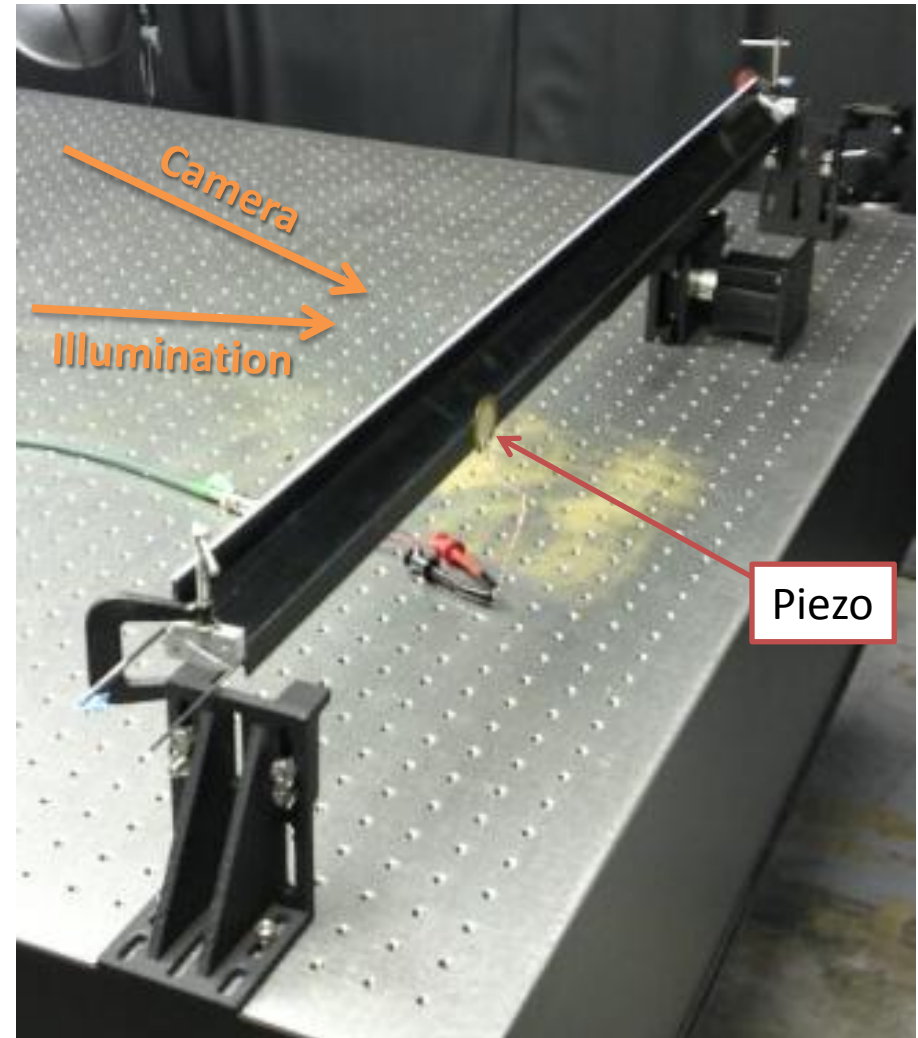
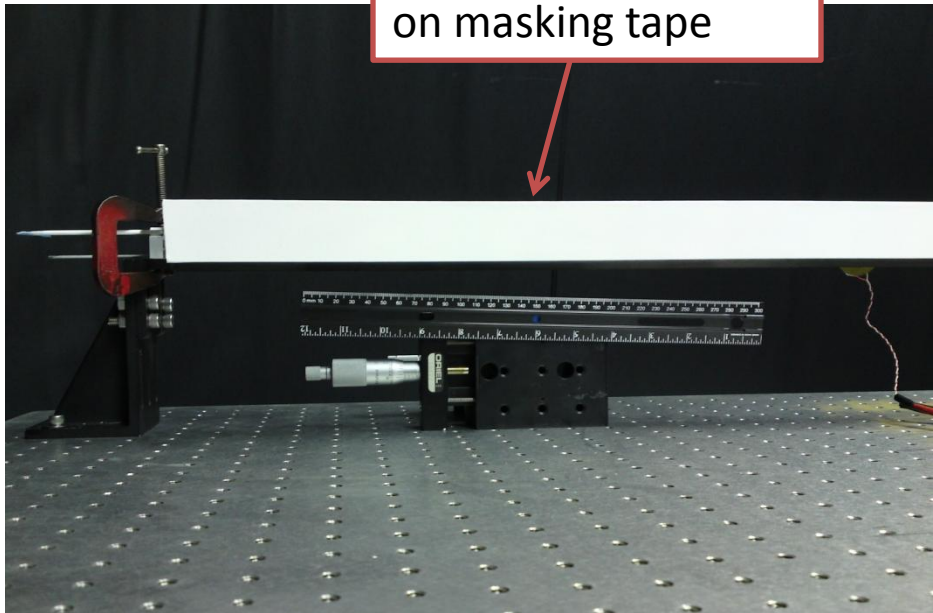


I-Beam Vibration Tests: TV Holography Setup

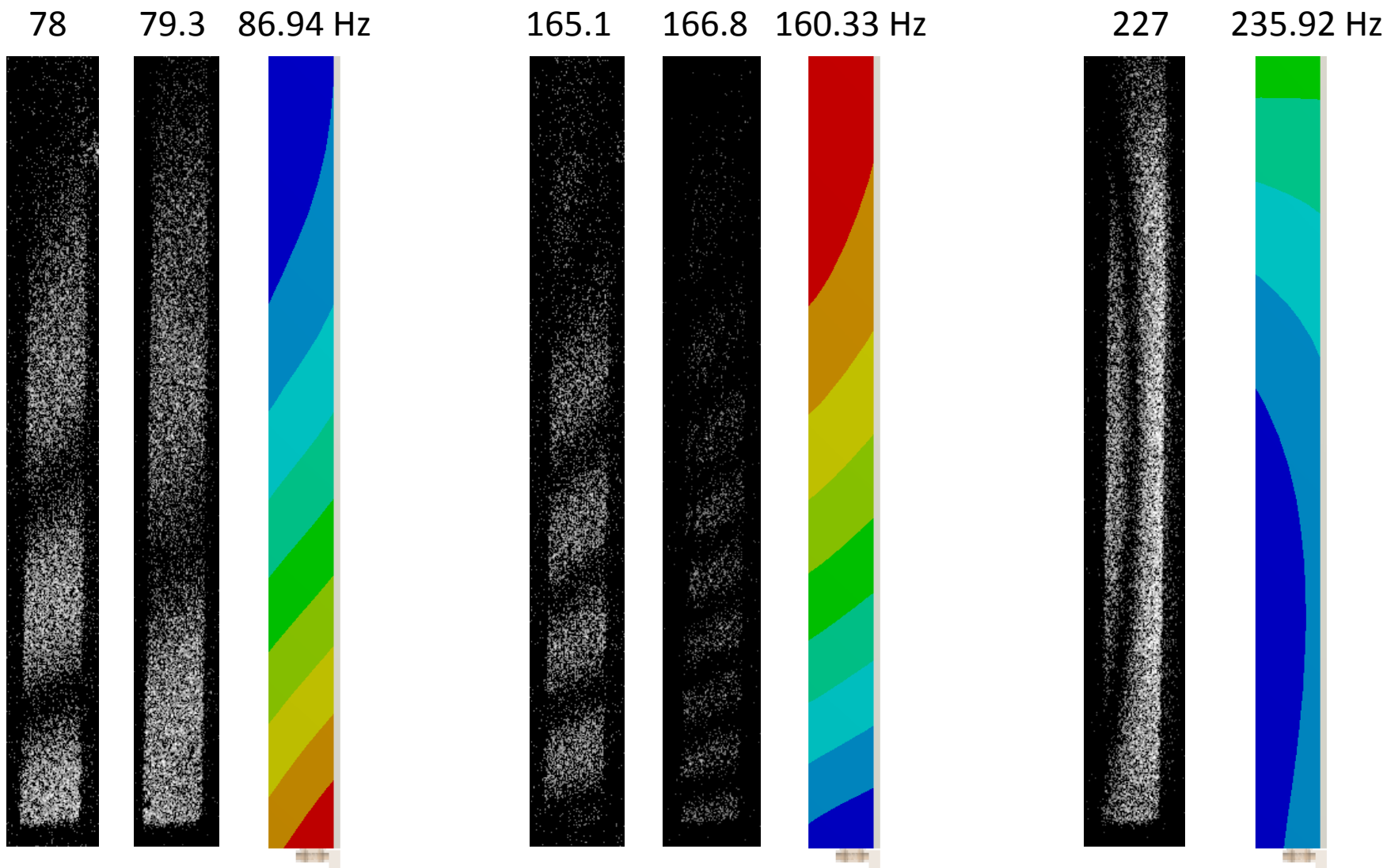
A few slides follow here which we can go through quickly...

Just to point out the usefulness of the TVH setup we have in 77A, for validating FEA.

Diffusing white paint on masking tape

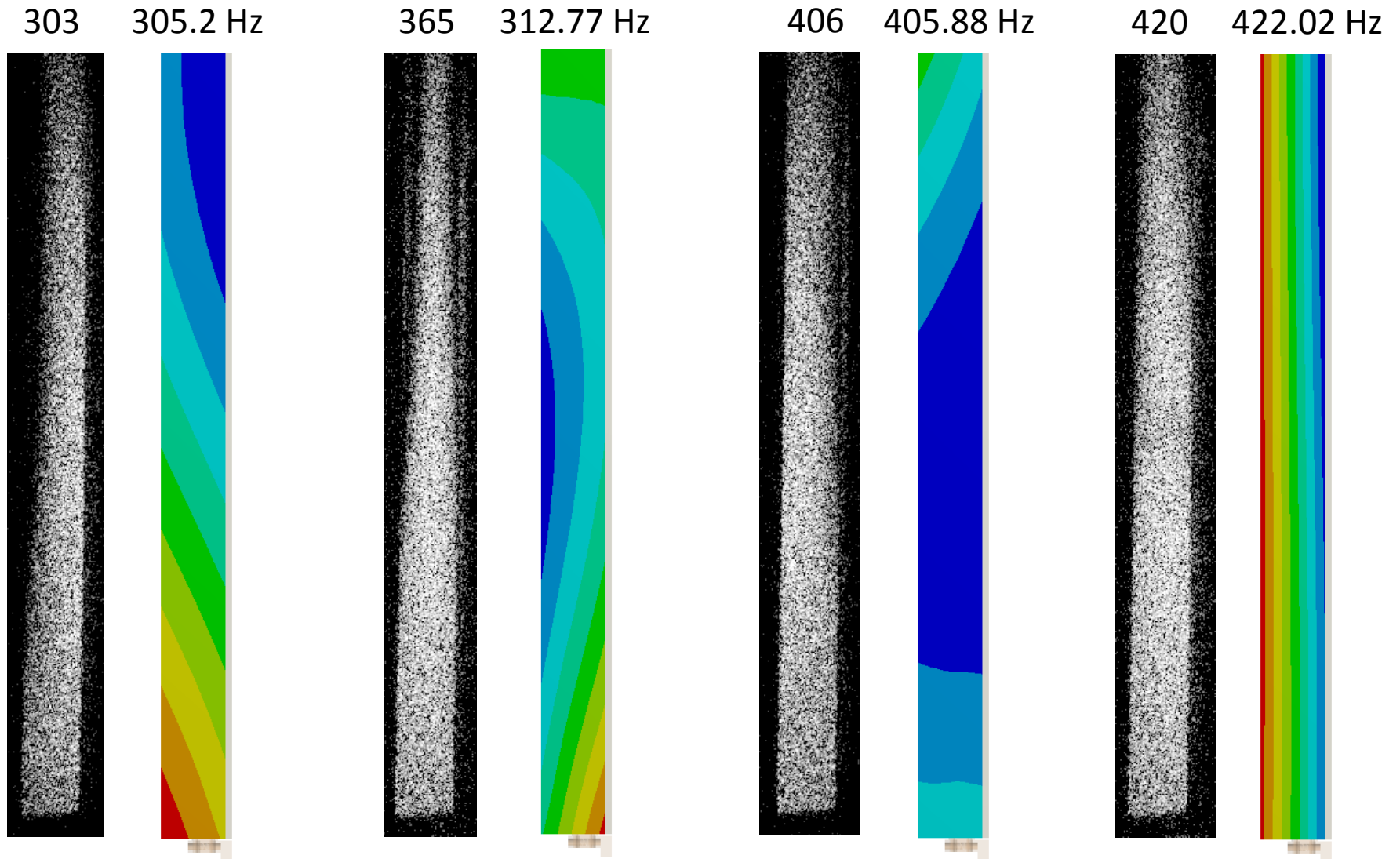


Vibration test results vs. FEA: 0 – 300 Hz



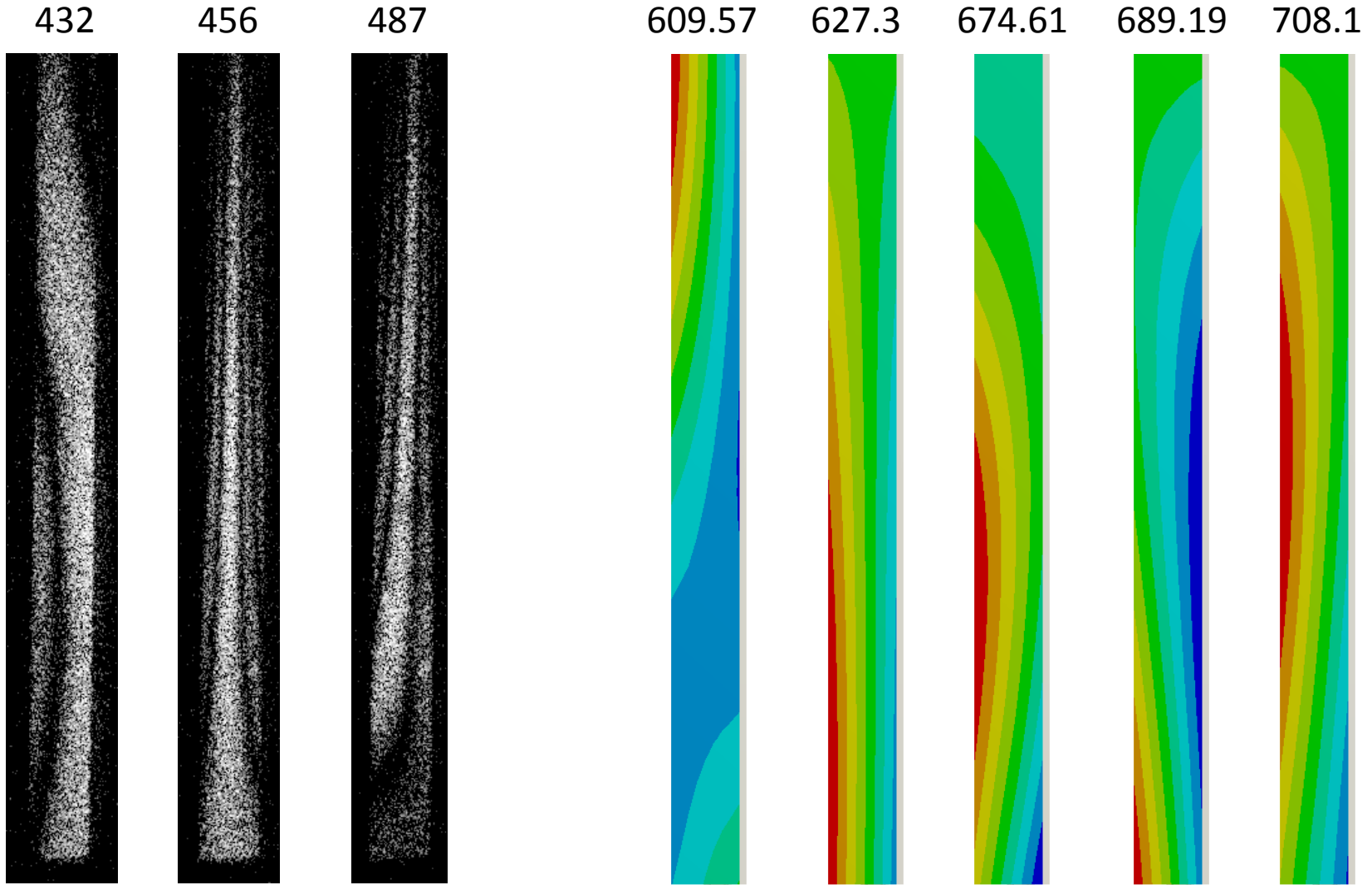
(All pictures show one half of the 1m I-Beam prototype / model.)

Vibration test results vs. FEA: 300 – 420Hz



Model did not resolve this early “wing” mode well.

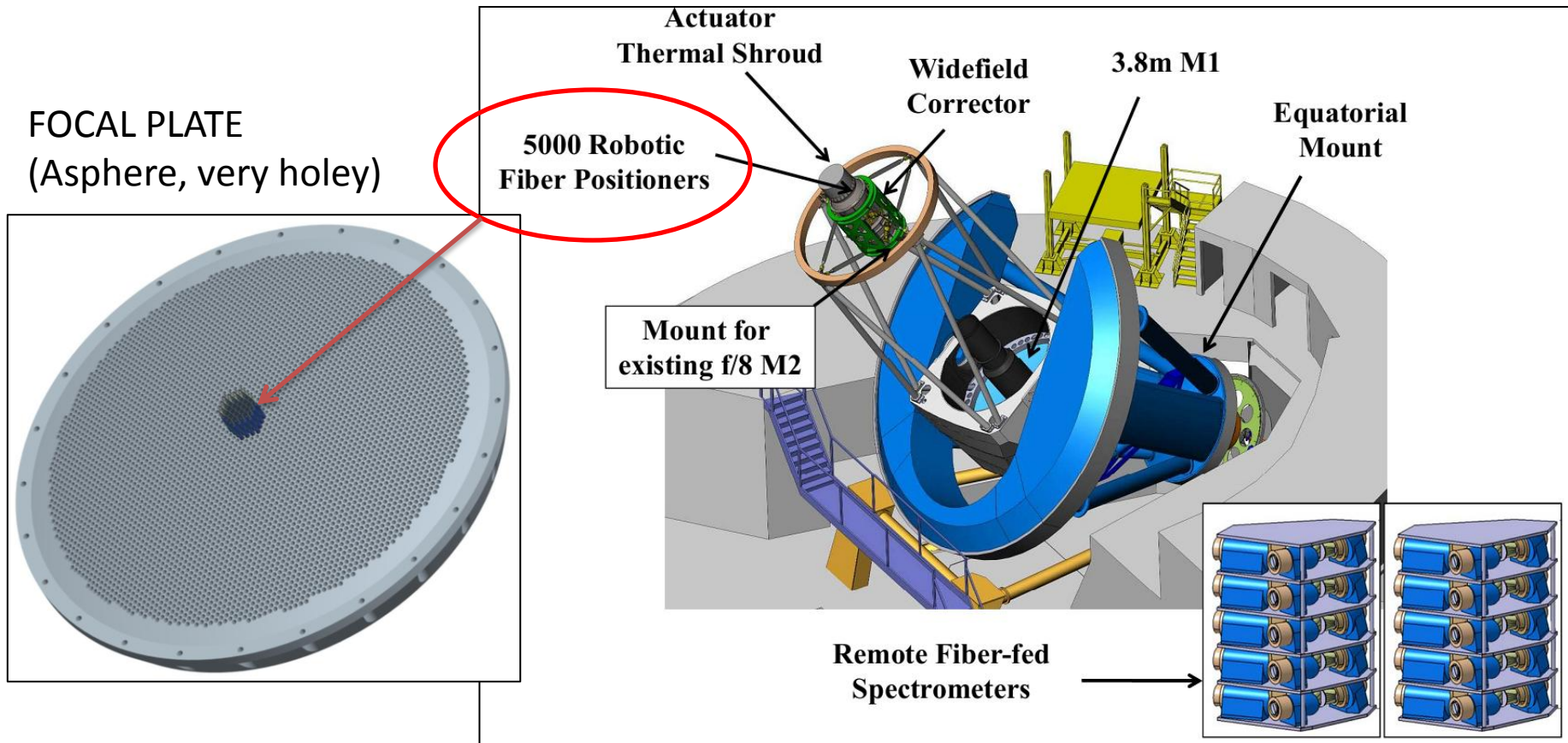
Vibration test results vs. FEA: Above 420 Hz



At $f > 420\text{Hz}$, Model decorrelates from actual frequencies, though similar clusters of mode shapes are seen. “Wing” shapes become prevalent – the absolute frequency values in this range are sensitive to properties of the foam core.

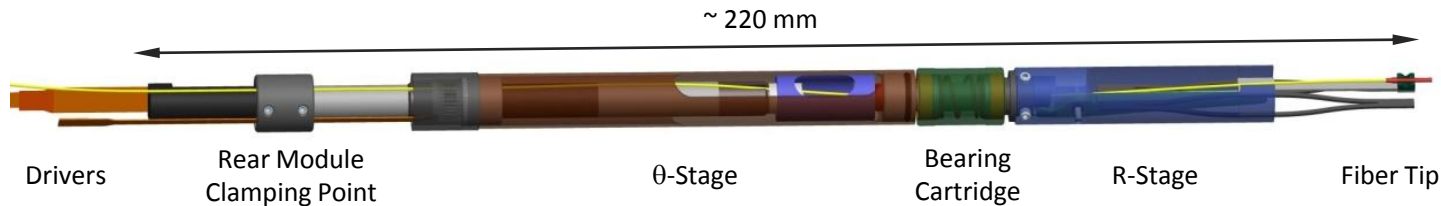
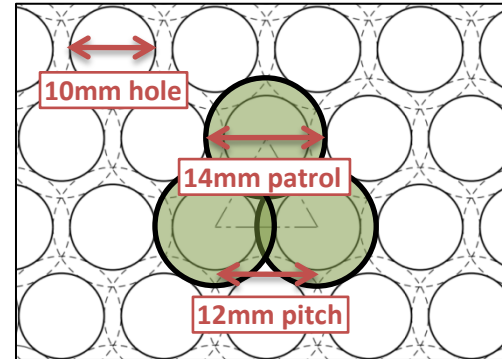
BigBOSS

- Multi-object spectrograph to be installed at Kitt Peak (Mayall 4m telescope)
- I've been principally involved with
 - Design/build/test of fiber positioners
 - Analysis of focal plate

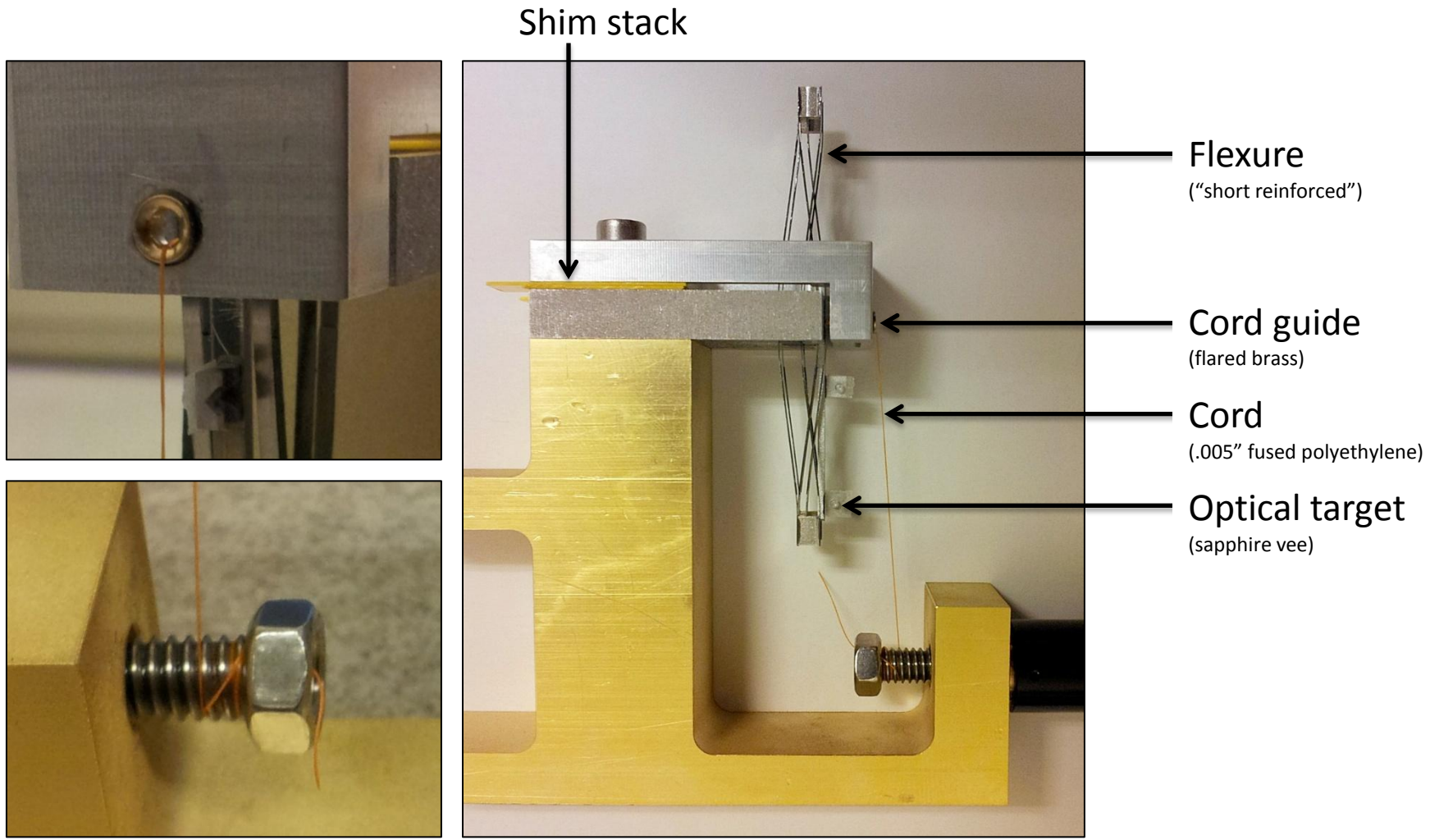


BigBOSS Fiber Positioner

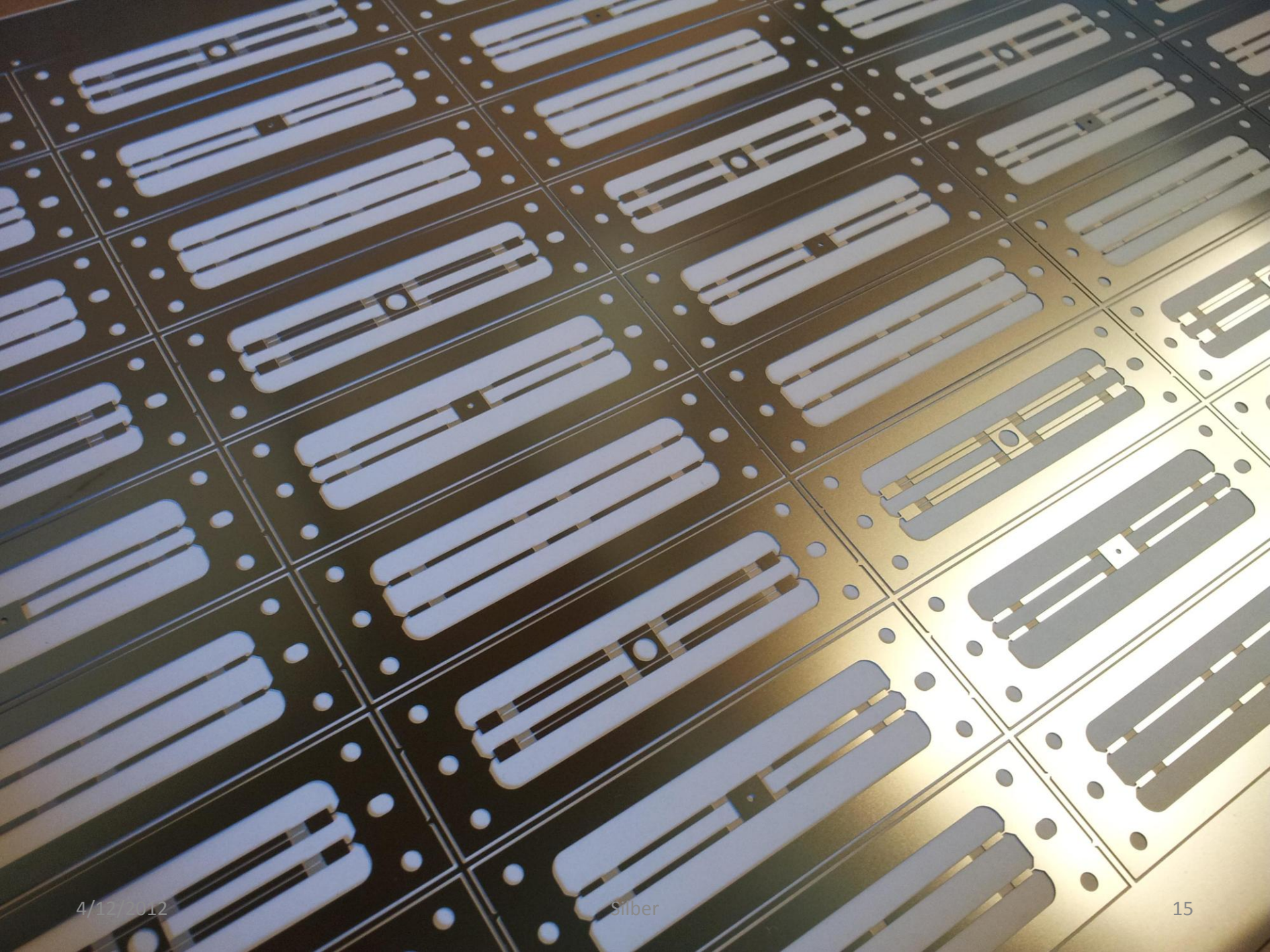
- 5000x individual robotic positioners, one for each fiber
- Demands high precision and stability in tight package
 - $\leq 5 \mu\text{m}$ in-plane precision
 - $\leq 40 \mu\text{m}$ in-plane absolute accuracy
 - $\leq 15 \mu\text{m}$ max deviation out-of-plane
 - $\leq 0.5^\circ$ total tilt deviation
- Testing of principle subcomponents (bearings, flexure) complete
- Assembly of first prototypes now complete, too
- As it happens, I'm doing the first tests of a fully integrated positioner this afternoon... very exciting!!
- Making a revised round of prototypes this month (will pull flexural R-Stage with a small cord, rather than pushing with a lever)



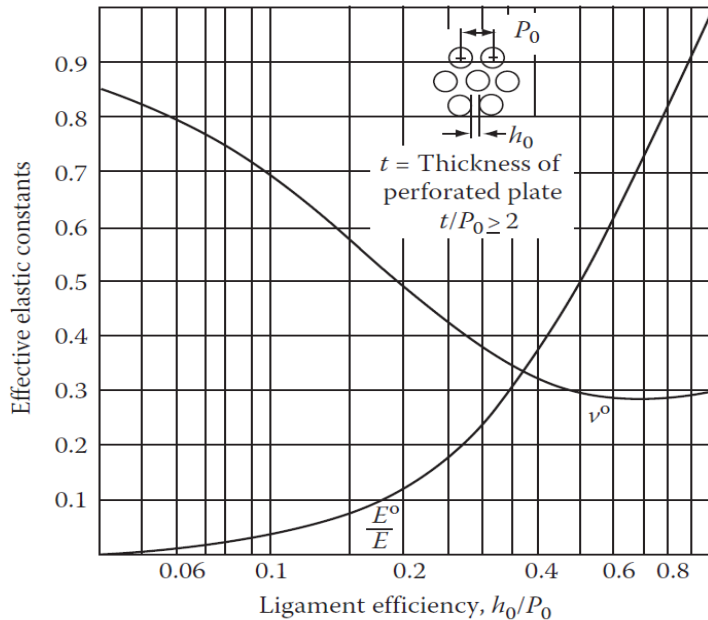
BigBOSS Fiber Positioner, Example of subcomponent test for flexural R-stage



Measured peak-peak parasitic error in this test was 8 μm over 8 mm travel



BigBOSS Focal Plate Equivalent Stiffnesses



Typical graph illustrating effects of perforation on elastic properties.

C.f. Osweiler, and other studies on in-plane properties of regularly perforated plates

Stiffness of the equivalent solid material is orthotropic – specifically, transversely isotropic (imagine a unidirectional fiber composite; the holes here are our “fibers”)

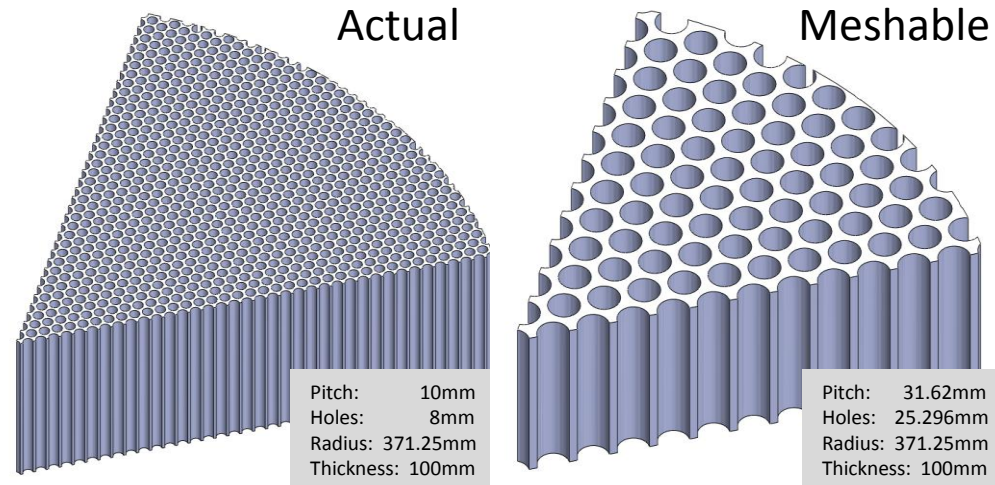
Name	Symbol	Unit	Verification Cases				
Plate Thickness	t	mm	100	100	100	100	100
Hole Pitch	p	mm	31.62	31.62	31.62	31.62	31.62
Hole Diameter	d_{hole}	mm	10	20	25.3	28	30
# Holes	N	#	500	500	500	500	500
	$E_x = (1 - f) * E_{plate}$	GPa	63.7	44.6	29.4	20.2	12.9
	$E_y = \eta * E_{plate}$	GPa	53.8	24.8	10.2	4.4	1.7
	$E_z = E_y$	GPa	53.8	24.8	10.2	4.4	1.7
	$\nu_{xy} = \nu_{plate}$	-	0.300	0.300	0.300	0.300	0.300
	$\nu_{yz} = \nu^*$	-	0.308	0.352	0.488	0.656	0.745
	$\nu_{xz} = \nu_{xy}$	-	0.300	0.300	0.300	0.300	0.300
	$G_{xy} = G^*$	GPa	24.5	17.2	11.3	7.8	4.9
	$G_{yz} = E_y / (2 * (1 + \nu_{yz}))$	GPa	20.5	9.2	3.4	1.3	0.5
	$G_{xz} = G_{xy}$	GPa	24.5	17.2	11.3	7.8	4.9

Verification Analyses

Multiple closed-form solutions (“hand calcs”) of flat circular plate

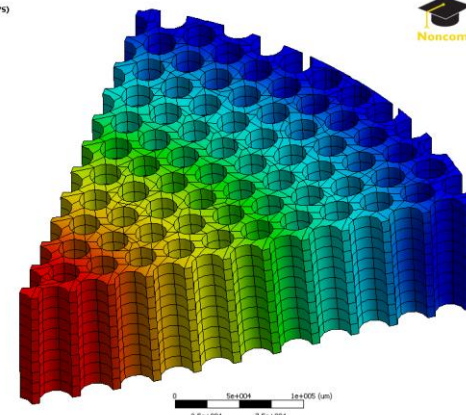
Multiple FEAs of flat perforated plate wedges with varying, large, hole patterns

Name	Unit	Verification Cases				
Plate Thickness	mm	100	100	100	100	100
Hole Pitch	mm	31.62	31.62	31.62	31.62	31.62
Hole Diameter	mm	10	20	25.296	28	30
# Holes	#	500	500	500	500	500
Plate Diameter	mm	742.5	742.5	742.5	742.5	742.5
Hole Area	mm ²	78.5	314.2	502.6	615.8	706.9
Ligament Width	mm	21.62	11.62	6.324	3.62	1.62
Ligament Efficiency	%	68.4%	36.7%	20.0%	11.4%	5.1%
Effective Modulus	%	76.8%	35.5%	14.6%	6.2%	2.5%
Effective Poisson's Ratio	-	0.308	0.352	0.4880	0.656	0.745
Plate Flexural Stiffness	N-m	4.9E+06	2.4E+06	1.1E+06	6.4E+05	3.2E+05
Effective Transverse Shear Modulus	N/m ²	2.4E+10	1.7E+10	1.1E+10	7.8E+09	4.9E+09
Hole Fraction	%	9.1%	36.3%	58.0%	71.1%	81.6%
Equiv Density for Solid Plate	kg/m ³	3163	4550	5660	6327	6863
Equiv Density for Perf Plate	μm	3478	7142	13490	21902	37373
Plate Mass	kg	137	197	245	274	297
Gravity Pressure	N/m ²	3103	4464	5553	6207	6733
Shear Deflection Component	μm	0.05	0.11	0.20	0.33	0.56
Total Center Deflection, built-in	μm	0.24	0.67	1.68	3.22	6.75
Total Center Deflection, simple support	μm	0.81	2.33	5.64	10.22	20.93



ANSYS Structural (ANSYS)
Plate
Type: Total Deformation
Unit: μm
Time: 1
10/12/2010 4:33:39H

1.6604 Max
1.4759
1.2814
1.1069
0.9243
0.7394
0.5546
0.3697
0.1849
0 Min



Verification Results

Hole Fraction	Ligament Efficiency (h/p)	E*/E	FEA - Perf Plate Distributed Mass	Spreadsheet "Hand" Calc	Orthotropic Equiv Solid FEA δ	Spreadsheet δ / Perf FEA δ	Equiv Solid FEA δ / Perf FEA δ
%	%	%	μm	μm	μm	-	-
9%	68%	77%	0.2382	0.2384	0.23583	1.00	0.99
36%	37%	35%	0.67717	0.6683	0.66727	0.99	0.99
58%	20%	15%	1.6604	1.6771	1.6972	1.01	1.02
71%	11%	6%	3.2287	3.2243	3.2618	1.00	1.01
82%	5%	2%	6.7954	6.7510	6.7664	0.99	1.00

So it was a nice way to capture material properties and make rapid design studies varying geometry and material for the focal plate.

This transversely isotropic formulation has not been tested yet, but "hand calcs" match up very closely to FEA for both solid and perforated FE models.

“Sale-able” skills for Eng Div

- Laminated composites analysis / design / production
- Low Z materials / structures
- Precision bonded assemblies
- Analysis / characterization of anisotropic materials
- Miniaturized actuators
- Precision flexure kinematics

End

Detail slides follow

PXL kinematic mounts, spring stiffnesses and FBD

Constant Stress "Tapered" Cantilever Spring
Nov 30, 2010

DESCRIBES THE CORRECT CONSTANT STRESS PROFILE

CONSTANT STRESS CONDITION:

$$\text{from } \sigma = \frac{My}{I} \Rightarrow \eta \sigma_y = \frac{M(x)y(x)}{I(x)}$$

$$\Rightarrow \eta \sigma_y = \frac{F(L-x)y(x)}{\frac{1}{2}b(2y(x))^3}$$

$$= \frac{3}{2} \frac{F}{b} \frac{L-x}{y(x)^2} \Rightarrow y(x) = \sqrt{\frac{3}{2} \frac{F}{\eta \sigma_y b} (L-x)}$$

SPECIFICATION OF $F = k\delta$ (SPRING CHARACTERISTICS):

$$\text{from } \delta = \frac{FL^3}{3EI}, \text{ approximate } I \approx \bar{I} = \int_0^L I(x) dx$$

$$\Rightarrow \frac{FL^4}{3E\delta} = \int_0^L \frac{1}{2}b(2y(x))^3 dx = \frac{3}{2}b \left(\frac{3}{2} \frac{F}{\eta \sigma_y b}\right)^{3/2} \int_0^L (L-x)^3 dx$$

$$= \frac{3}{2}b \left(\frac{3}{2} \frac{F}{\eta \sigma_y b}\right)^{3/2} \left(-\frac{1}{4}(L-x)^4\right) \Big|_0^L = \frac{4}{15}b \left(\frac{3}{2} \frac{F}{\eta \sigma_y b}\right)^{3/2} L^{5/2}$$

$$\Rightarrow L^{3/2} = \frac{15}{4} \frac{E\delta}{F} b \left(\frac{3}{2} \frac{F}{\eta \sigma_y b}\right)^{3/2} = \frac{4}{5} E\delta F^{1/2} b^{-1/2} \left(\frac{3}{2} \frac{1}{\eta \sigma_y}\right)^{3/2}$$

$$\Rightarrow L = \left(\frac{4}{5} E\delta \left(\frac{F}{b}\right)^{1/2}\right)^{2/3} \frac{3}{2} \frac{1}{\eta \sigma_y}$$

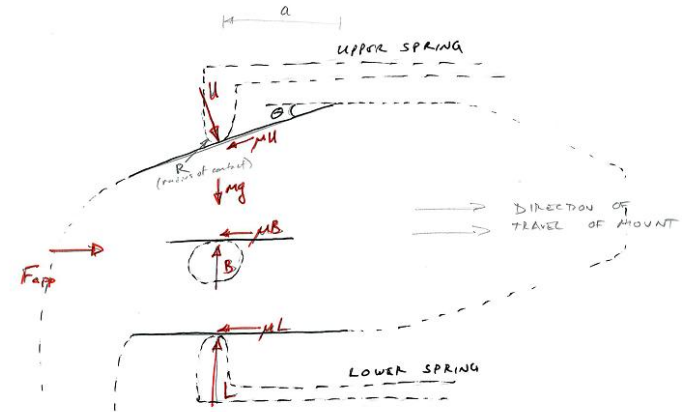
$$\Rightarrow L = \frac{3}{2} \frac{1}{\eta \sigma_y} \left(\frac{4}{5} E\delta\right)^{2/3} \left(\frac{F}{b}\right)^{1/3} *$$

SETS THE REQUIRED BEAM LENGTH FOR A SPECIFIED COMBINATION OF

$\eta \sigma_y$ = max fraction of yield stress
 E = modulus
 δ = max deflection
 F = max force
 b = beam width

* Note that this design analysis tends to under predict δ by about 15%. Thus, it may be useful to replace δ with $\delta^* = C \delta_{\text{desired}}$, where $C \approx 1.15$

FBD FOR KEY CONDITIONS AT END OF KINEMATIC MOUNT RUN



HORIZONTAL: $F_{app} = \mu L + \mu B + (\mu \cos \theta - \sin \theta) U$ ①

VERTICAL: $Mg = L + B - (\mu \sin \theta + \cos \theta) U$ ②

SPRING FORCES: $L = k_L \delta_L$
 $U = k_U \delta_U / \cos \theta$

② $\Rightarrow B = Mg - k_L \delta_L + (\mu \tan \theta + 1) k_U \delta_U$

① $\Rightarrow F_{app} = \mu k_L \delta_L + \mu B + (\mu - \tan \theta) k_U \delta_U$

PLUS SIGN FOR ALTERNATE CASE

MAX BALL CONTACT FORCE CHECK: Let $\delta_U = \delta_{U,max}$, and conservatively keep the exit angle (no radius at transition).

SELF-SLIP CONDITION AT EXIT: Let $\delta_U = \delta_{U,max} - \beta$ and see whether $F_{app} < 0$ (indicating self-slip).

NOTE: $g = R(1 - \sin \theta \tan \theta - \cos \theta) + a \tan \theta$

PXL kinematic mounts, FBD calculations

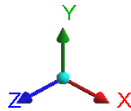
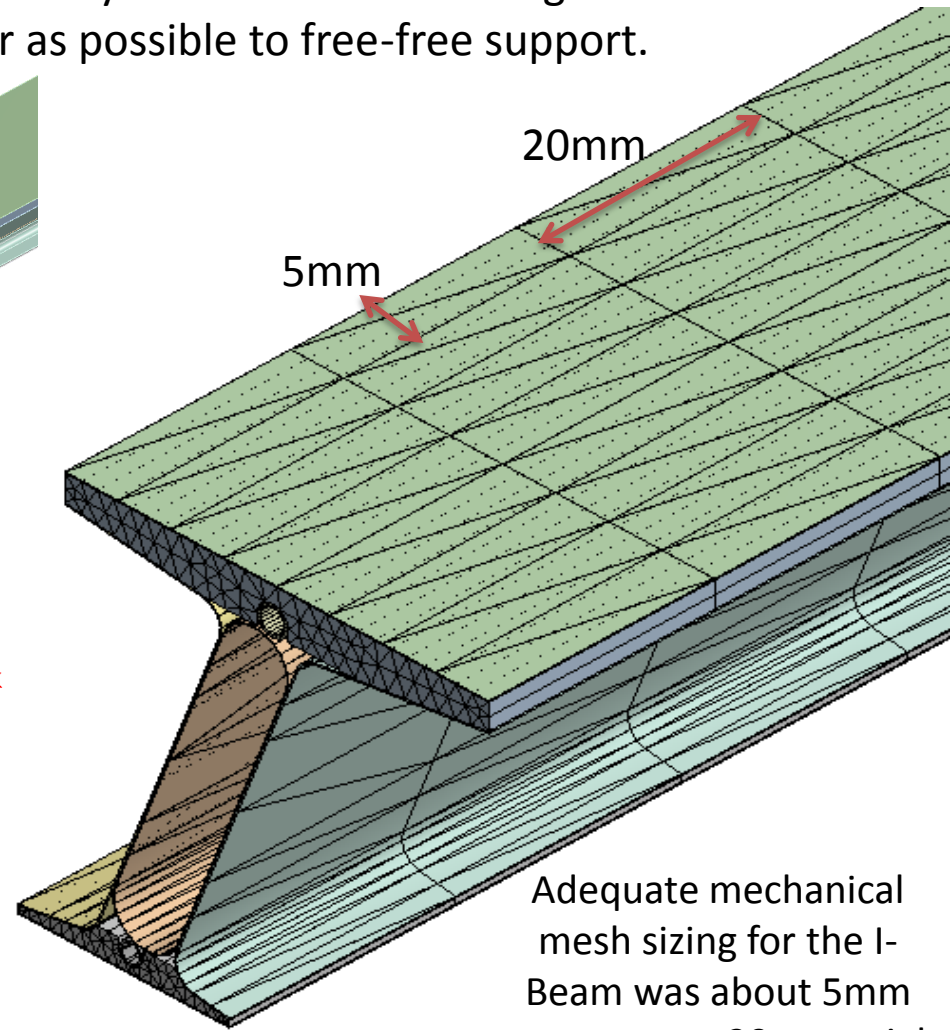
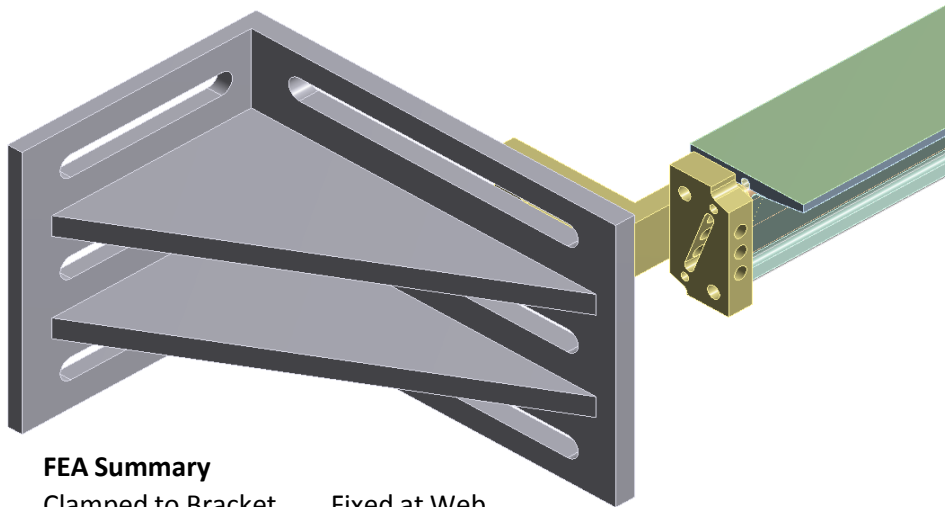
PARAMETERS			
static friction coefficient	mu	-	0.2
exit angle of upper spring contact	ang	deg	45
exit angle of upper spring contact	ang	rad	0.785
final distance past start of exit angle	a	mm	1.00
radius of upper spring contact	rUmax	mm	1.59
spring constant at top mount's upper surface	kU	N/mm	7.5
max deflection of top mount's upper spring	dUmax	mm	2.0
final deflection of top mount's upper spring	dUfinal	mm	1.658
spring constant at top mount's lower surface	kL	N/mm	11.2
max deflection of top mount's lower surface	dLmax	mm	1.75
spring constant at bottom mount	kB	N/mm	10.0
max deflection of bottom mount's spring	dBmax	mm	0.5
supported mass	m	kg	2.5
supported weight	mg	N	24.5
TOP EAST KIN MOUNT			
ball contact force at end of travel	Bfinal	N	19.8
max ball contact force during travel (conservative)	Bmax	N	22.9
max upper spring contact force during travel	Umax	N	15
max lower spring contact force during travel	Lmax	N	19.6
max insertion force during travel	Fappmax	N	18.4
insertion force at end of travel (negative --> self-slip)	Fappfinal	N	-2.1
retraction force at end of travel	Fretfinal	N	22.8
TOP WEST KIN MOUNT			
ball contact force at end of travel	Bfinal	N	14.9
max ball contact force during travel (conservative)	Bmax	N	18.0
max upper spring contact force during travel	Umax	N	15
max lower spring contact force during travel	Lmax	N	0.0
max insertion force during travel	Fappmax	N	9.6
insertion force at end of travel (negative --> self-slip)	Fappfinal	N	-7.0
retraction force at end of travel	Fretfinal	N	21.8
BOTTOM KIN MOUNT			
max ball contact force during travel (conservative)	Bmax	N	5.0
max insertion force during travel	Fappmax	N	1.0
TOTAL			
max insertion force during travel	Fappmax	N	29.0
insertion force at end of travel (negative --> self-slip)	Fappfinal	N	-8.0
retraction force at end of travel	Fretfinal	N	45.6

PXL kinematic mounts, contact stress calcs

Sphere-on-Cylinder Contact																					
BALL			GROOVE																		
E1	nu1	D1	E2	nu2	R2	D2	Syc2	V1	V2	Q	A/B	1/A	-1/e dE/dE	a	theta	F (applied)	F	Pmax	~Taumax	~FOS2 (tresca)	
GPa	-	mm	GPa	-	mm	mm	MPa	1/Pa	1/Pa	1/Pa	-	m	-	mm	deg	N	N	MPa	MPa	-	
345.0	0.24	3.97	113.8	0.34	-2.50	-5.00	880	8.7E-13	2.5E-12	2.5E-12	0.206	0.019	1.5450	0.138	45	25.0	17.7	443	133	3.31	
345.0	0.24	12.70	113.8	0.34	1E+06	2E+06	880	8.7E-13	2.5E-12	2.5E-12	1.000	0.013	0.7854	0.063	n/a	5.0	5.0	602	181	2.44	
The value -1/e dE/de is from a lookup table (Puttock and Thwaite 1969).																					
Cylinder-on-Plane Contact																					
SPRING CONTACT			GUIDE SURFACE					WIDTH													
E1	nu1	D1	E2	nu2	R2	D2	Syc2	L	b	F	Pmax	~Taumax	~FOS2 (tresca)								
GPa	-	mm	GPa	-	mm	mm	MPa	mm	mm	N	MPa	MPa	-								
113.8	0.34	3.18	300.0	0.21	1E+06	2E+06	880	4.50	0.011	25.0	319	96	4.60	Alumina							
113.8	0.34	3.18	200.0	0.32	1E+06	2E+06	880	4.50	0.012	25.0	302	90	4.86	Zirconia							

I-BEAM VIBRATION FEA: FEA Details

Test measurement was quite sensitive to boundary condition of mounting bracket.
In future, would suspend beam to get as near as possible to free-free support.



FEA Summary

Clamped to Bracket

Mode	Freq
1	86.944
2	160.33
3	235.92
4	305.2
5	312.77
6	405.88
7	422.02
8	609.57
9	627.3
10	674.61
11	689.19
12	708.1

Fixed at Web

Mode	Freq
1	102.59
2	282.06
3	322.56
4	435.54
5	650.91
6	654.15
7	770.18
8	971.74
9	1042.6
10	1275.9
11	1315.8
12	1447.4

Adequate mechanical mesh sizing for the I-Beam was about 5mm transverse x 20mm axial

I-BEAM VIBRATION FEA: Material Properties Used

Material	Density	FAW	CPT	E1	E2,E3	G12,G13	G23	v12, v13	v23
-	<i>kg/m³</i>	<i>g/m²</i>	<i>μm</i>	<i>GPa</i>	<i>GPa</i>	<i>GPa</i>	<i>GPa</i>	-	-
K13C2U	1762	46	35.9	522	5.8	6.7	1.8	0.319	0.621
M46J	1553	30	28.7	255	6.6	6.6	2.1	0.279	0.559
K9 Allcomp Foam	230	-	-	0.29	-	-	-	0.3	-

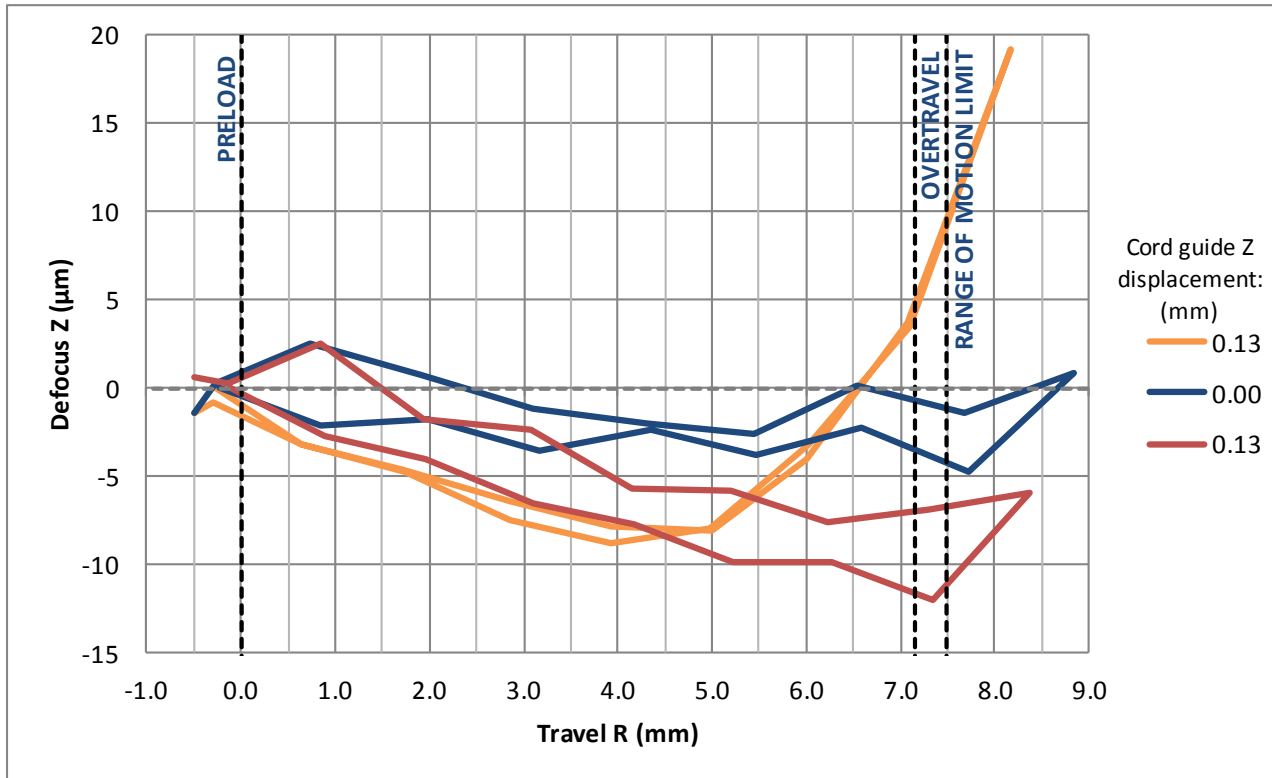
I calculated all ply properties from micromechanics following Kollar and Springer, inputting fiber and resin properties from the respective vendors, with 58% volume fraction and 0.5% void fraction.

CPTs calculated from inputs of FAW, resin content, volume fractions, and densities. This method gave CPTs within 5% of measured values for the 98gsm K13C2U laminate we're using in the STAR Inner Detector Support.

Note that Tencate (pregregger) made a series of tensile test samples off the roll of 46gsm K13C2U used here, and measured a 0° tensile modulus ranging between 511 – 587 GPa, with a lot average of 536 GPa.

2012-02-24 Cord Test

Defocus results

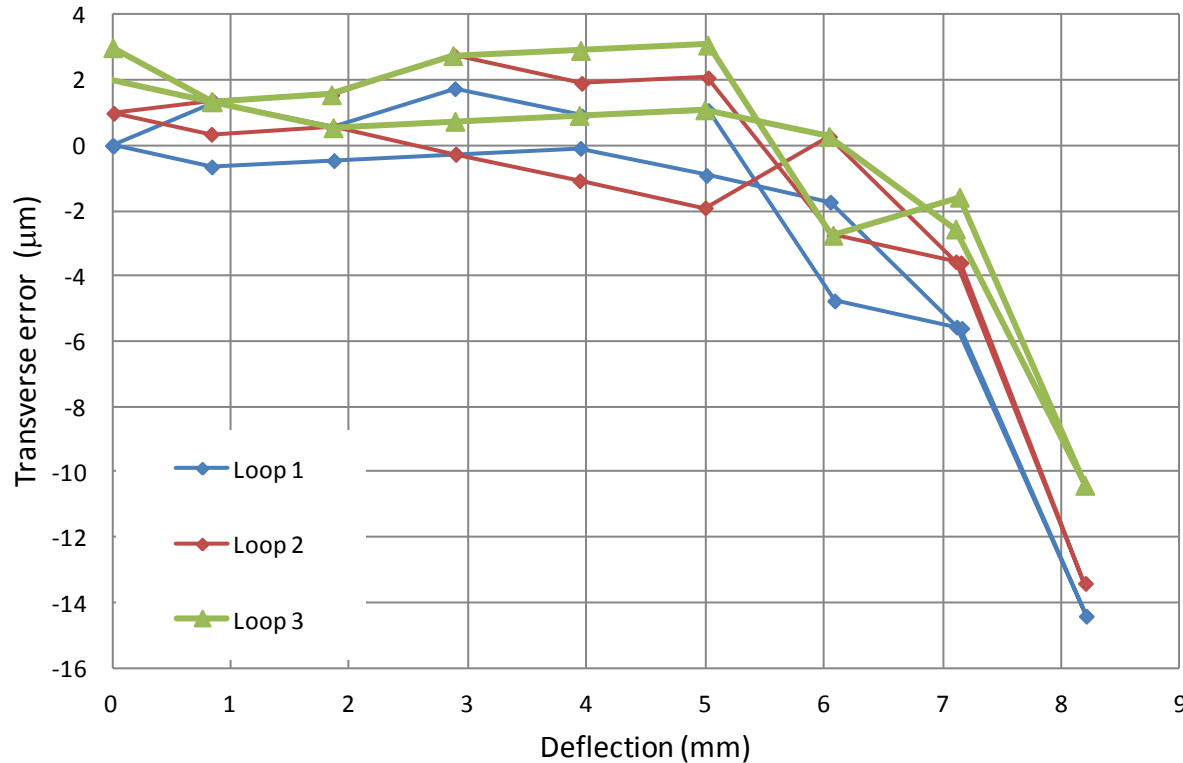


Comments:

- Cord guide was shimmed up/down in Z by .005" increments.
- Location of Z = zero displacement is nominal, may be off by up to .002".
- Flexure had been glued to mount non-perpendicular by 0.23°. This and the mount's angle with respect to smartscope bed have been rotated out.

2012-02-24 Cord Test

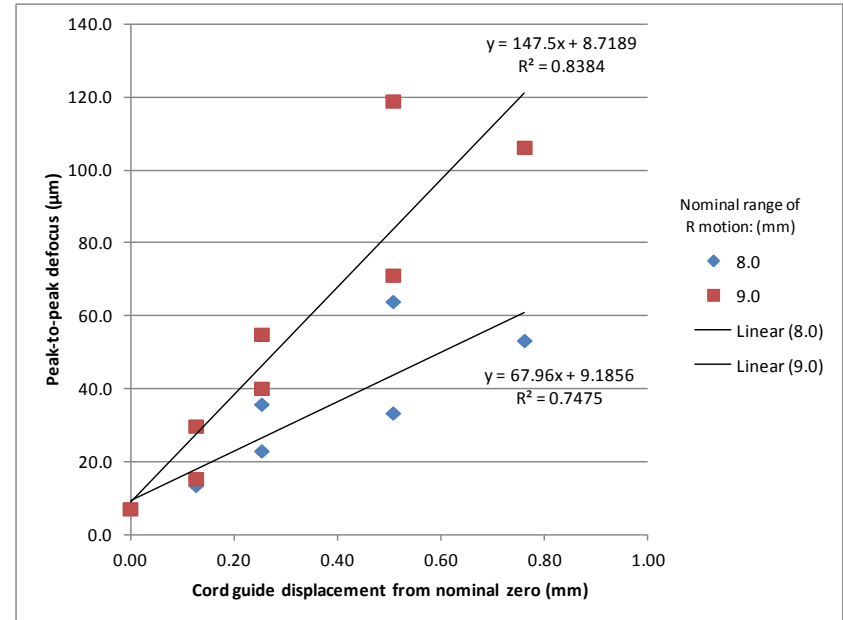
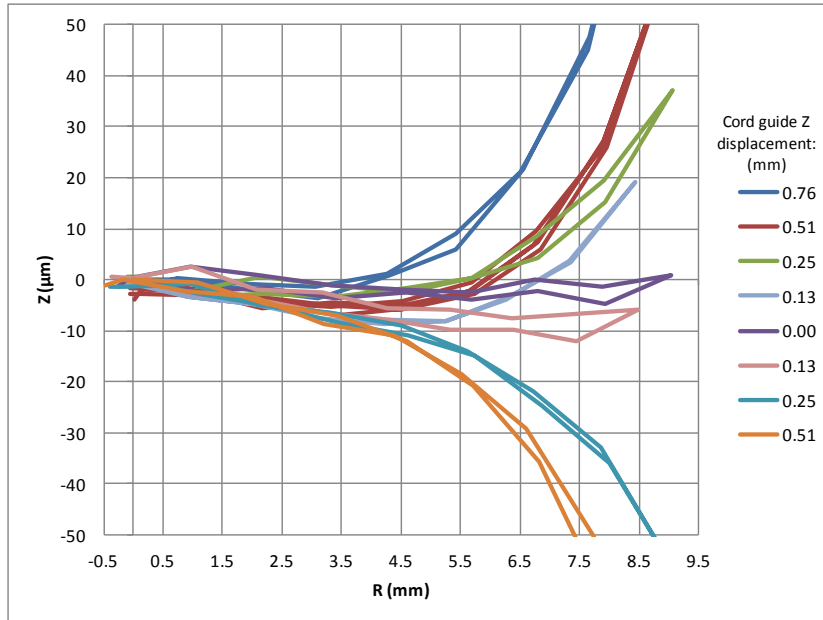
Transverse results



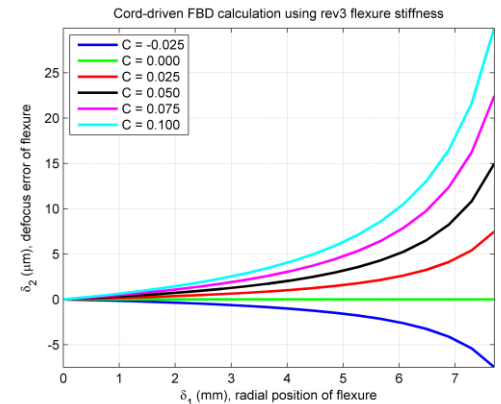
Comments:

- Shim stack same as for nominal Z = zero of defocus measurements
- No ability in test setup to adjust guide position in the T direction, hence:
 - Trend in data towards -T
 - No data to assess sensitivity to guide placement error

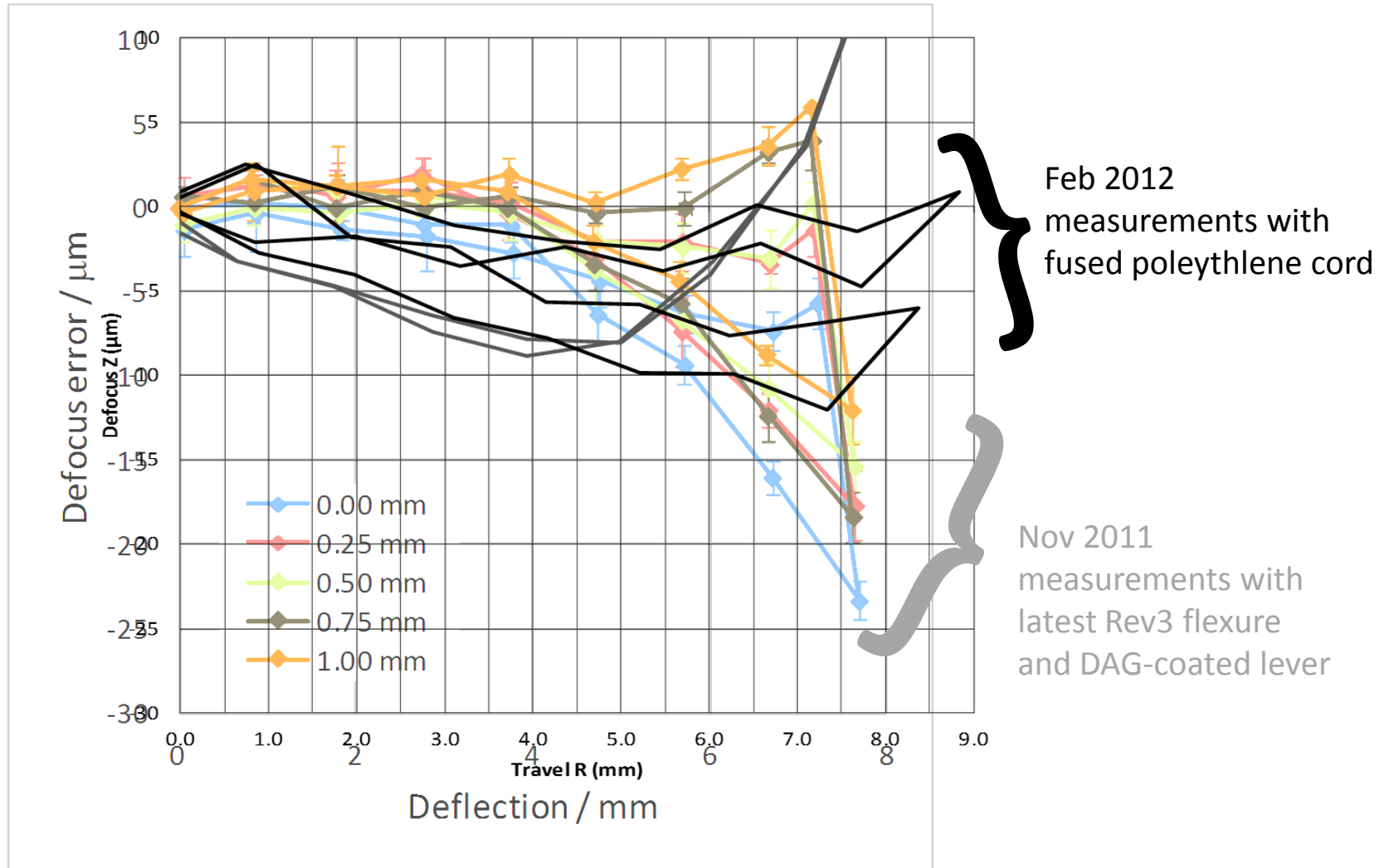
Defocus sensitivity



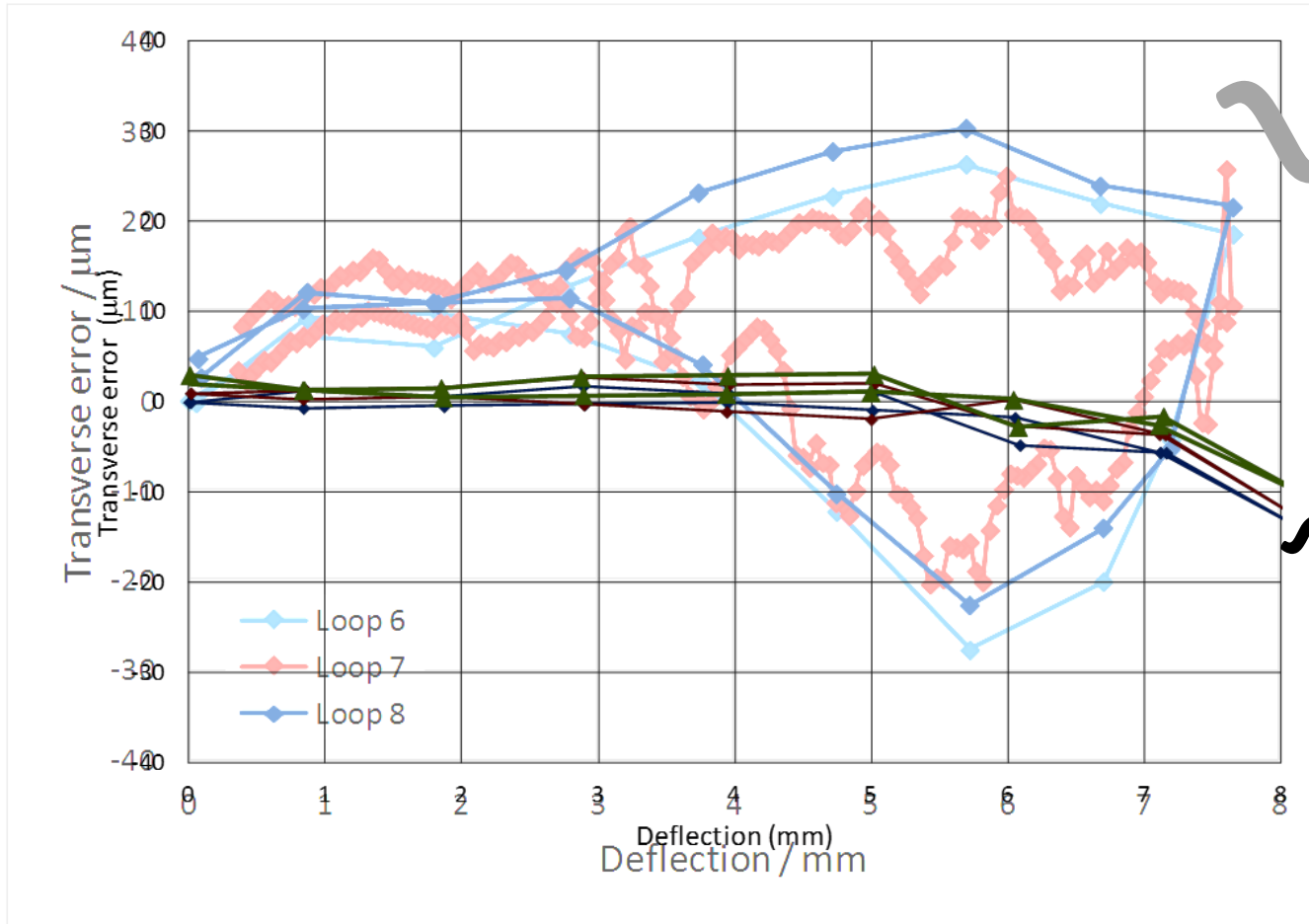
- Exaggerate displacements of cord guide to assess sensitivity.
- FBD estimate (2011-01-25) was 15µm defocus (30µm peak-to-peak) per 50µm displacement error of guide
- Linear fit on measured peak-to-peak defocus vs guide displacement to assess measured sensitivity. Much lower than the FBD estimate:
 - Over 8mm of travel: 3.4µm defocus / 50µm guide offset
 - Over 9mm of travel: 7.4µm defocus / 50µm guide offset



Comparison with lever test: Defocus



Comparison with lever test: **Transverse**

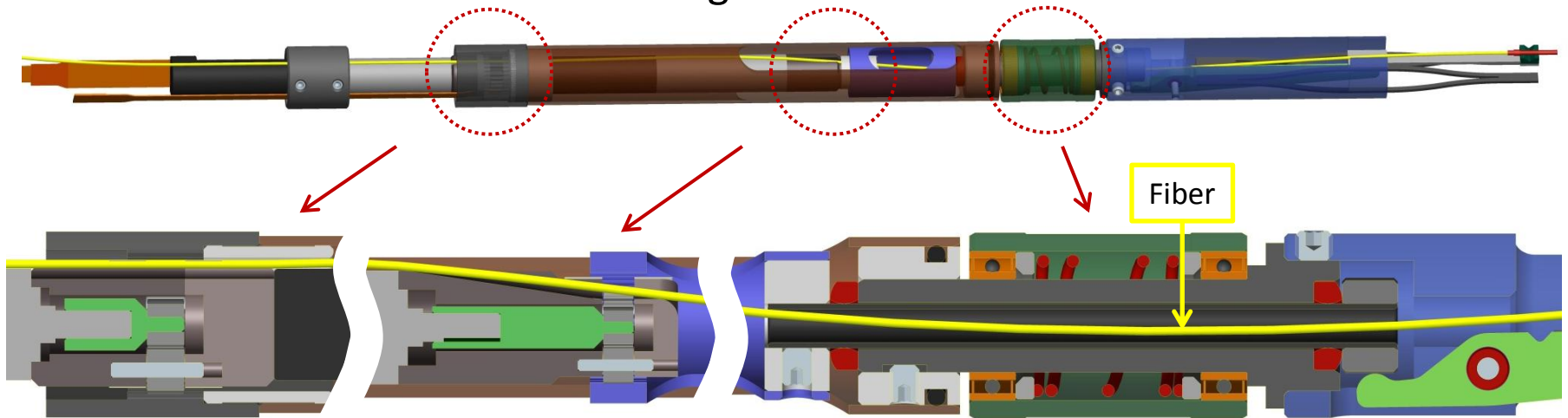


Nov 2011
measurements with
latest Rev3 flexure
and DAG-coated lever

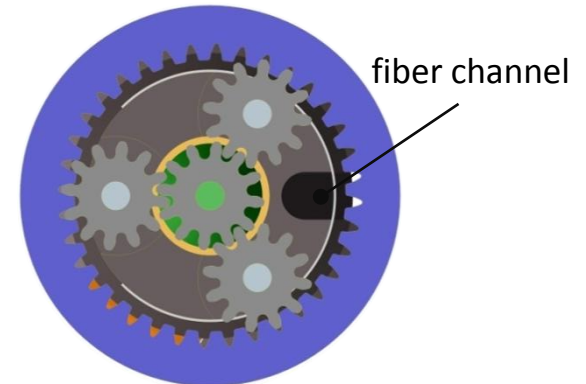
Feb 2012
measurements with
fused polyethylene cord

BigBOSS Positioner Fiber Path

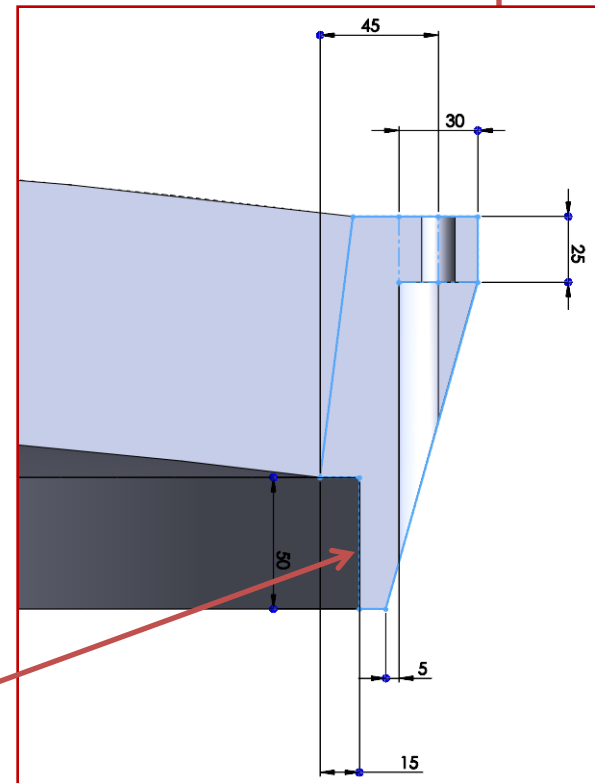
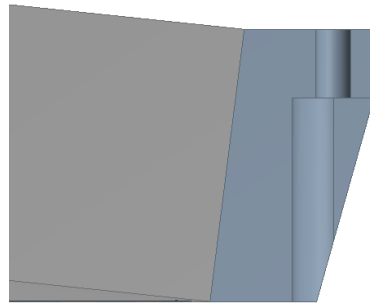
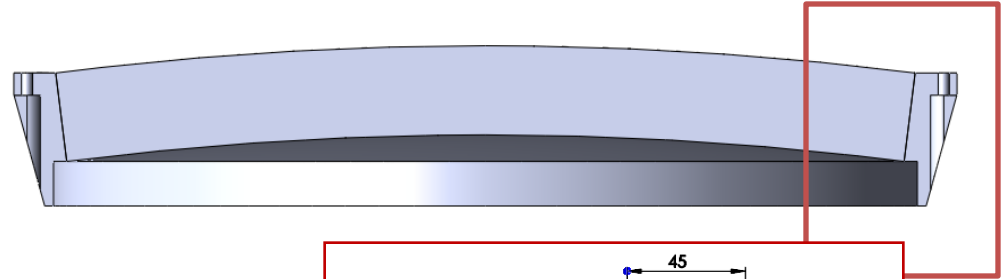
- Fiber runs sideways along the rear module, laterally constrained by channels to avoid collisions with gears



- transfer gear similar to planetary gear but with *pinned* planets allows bypass channels for fiber and wires
- easy penetration of rotational mechanical coupling with 360° freedom



Typical Geometry

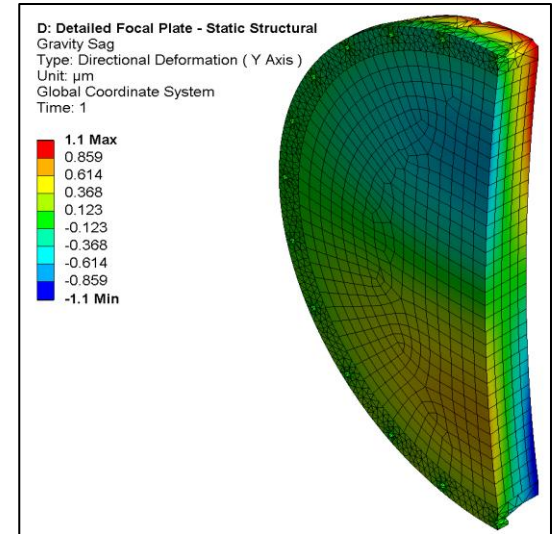
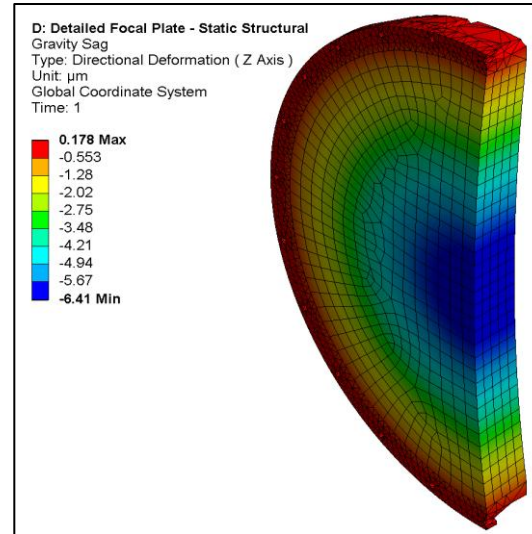


Lopped-off rim

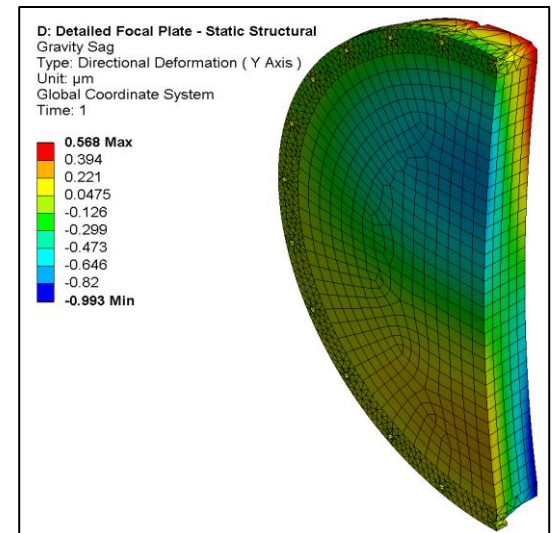
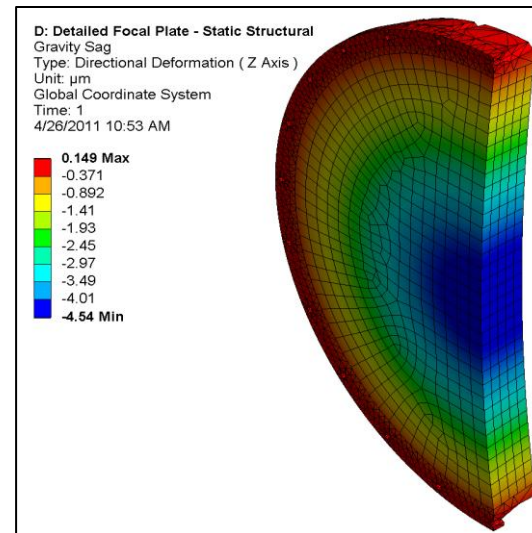
Extended rim

Typical FEA Results

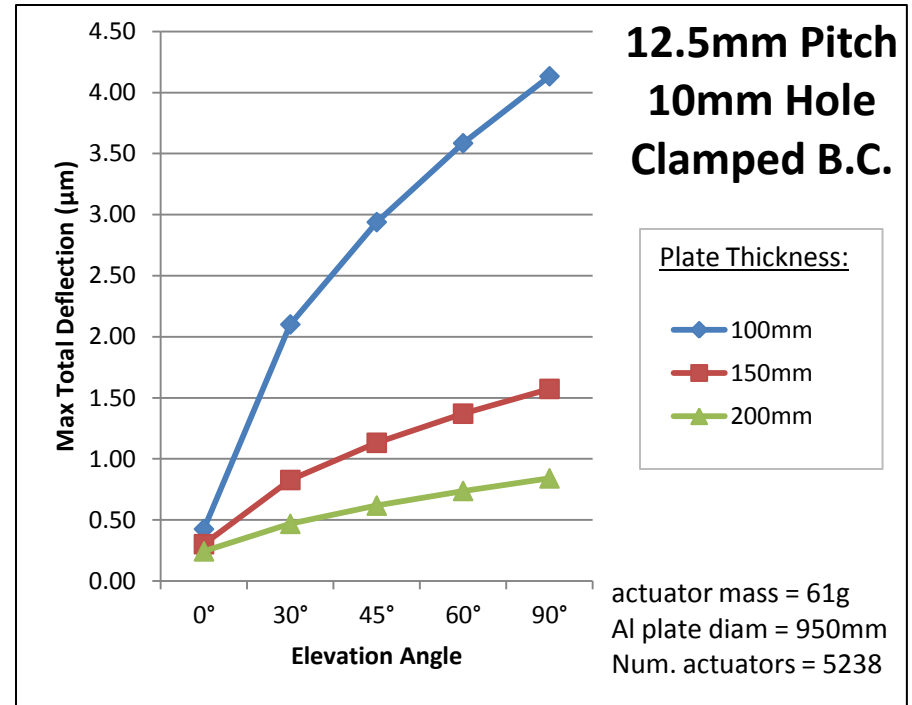
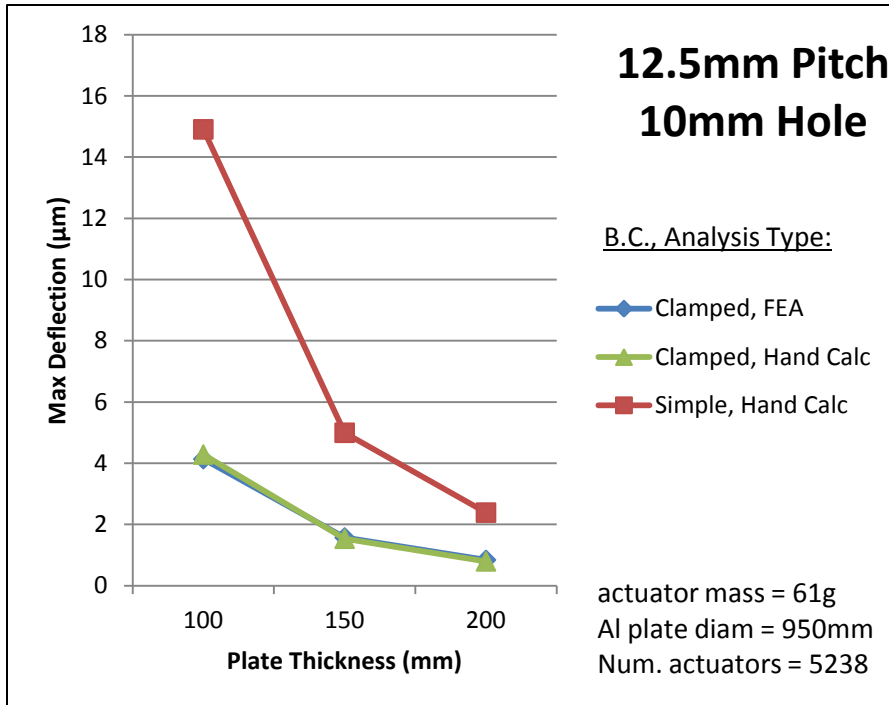
Elevation Angle: 90°
Material: Steel
Thickness: 100mm
Pitch: 12mm
Diam: 10mm



Elevation Angle: 45°
Material: Steel
Thickness: 100mm
Pitch: 12mm
Diam: 10mm



Typical Trends



Summary of Results

(2600mm Focal Surface, 90° Elevation Angle)

Description	Mass* (kg)	Modulus / Mass (GPa/kg)	Total Deflection (μm)
Aluminum, Extended Rim	481	0.15	11.4
Aluminum, Lopped-off Rim	474	0.15	13.5
CE7 Al-Si, Extended Rim	469	0.28	6.0
CE7 Al-Si, Lopped-off Rim	462	0.28	7.2
Steel, Extended Rim	701	0.29	5.4
Steel, Lopped-off Rim	680	0.29	6.4

*Mass includes 5000x positioners, 61.3g each.

Description	Total Deflection (μm)	
	<i>Simple</i>	<i>Built-In</i>
Spreadsheet Calc, Aluminum	17.7	5.2
Spreadsheet Calc, CE7 Al-Si	9.4	2.8
Spreadsheet Calc, Steel	8.4	2.5

Roughly equivalent deflection performance between steel and CE7. Assuming a precipitation-hardened stainless, the biggest tradeoff is between strength of steel (~10x better) versus thermal conductivity of CE7 (~10x better).